The color dipole picture

Dieter Schildknecht

Fakultät für Physik, Universität Bielefeld

& Max Planck Institut für Physik, München

Diffraction 2012

Puerto del Carmen, Lanzarote, Canary Islands (Spain),

September 10 – September 15, 2012

1. Introduction

The concepts of "color transparency" and "saturation".

Deep inelastic scattering (DIS), HERA 1992 to 2007:

DIS at low values of

$$x \equiv x_{bj} \simeq \frac{Q^2}{W^2}, \text{ where}$$

$$5 \cdot 10^{-4} \leq x \leq 10^{-1}$$

$$0 \leq Q^2 \leq 100 GeV^2$$

Low-x Scaling

$$\text{Empirically}: \qquad \eta(W^2, Q^2) \equiv \frac{Q^2 + m_0^2}{\Lambda_{sat}^2(W^2)}$$

$$\Lambda_{sat}^2(W^2) \sim (W^2)^{C_2}$$

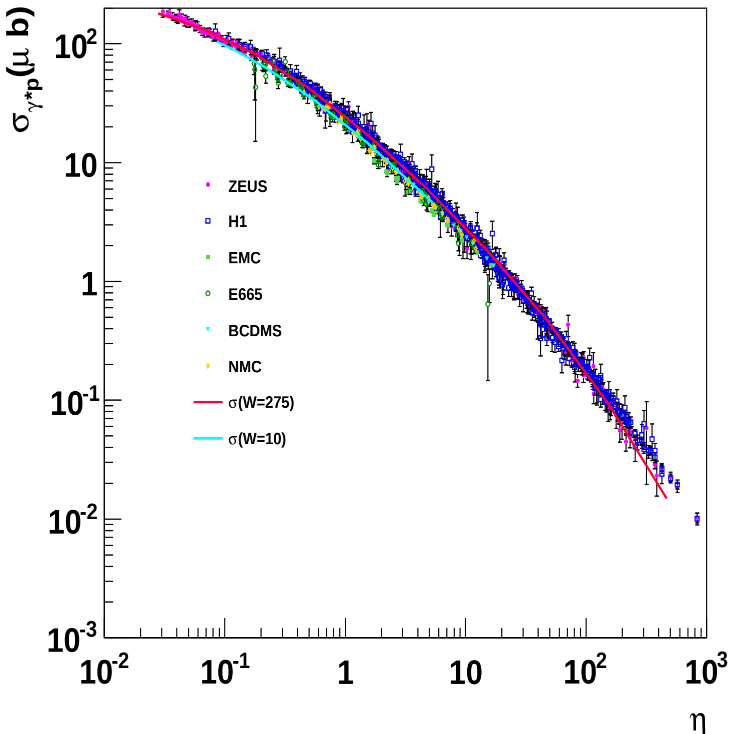

Schildknecht, Surrow, Tentyukov (2000)

$$\begin{aligned}\sigma_{\gamma^* p}(W^2, Q^2) &= \sigma_{\gamma^* p}(\eta(W^2, Q^2)) \\ &\sim \sigma^{(\infty)} \begin{cases} ln\frac{1}{\eta(W^2,Q^2)} & , \quad \text{for } \eta(W^2, Q^2) \ll 1 \\ \frac{1}{\eta(W^2,Q^2)} & , \quad \text{for } \eta(W^2, Q^2) \gg 1 \end{cases}\end{aligned}$$

The limit of $\eta(W^2, Q^2) \to 0$, or $W^2 \to \infty$ at Q^2 fixed

$$\lim_{\substack{W^2\to\infty \\ Q^2 \text{ fixed}}} \frac{\sigma_{\gamma^* p}(\eta(W^2,Q^2))}{\sigma_{\gamma^* p}(\eta(W^2,Q^2=0))} = \lim_{\substack{W^2\to\infty \\ Q^2 \text{ fixed}}} \frac{\ln\left(\frac{\Lambda^2_{sat}(W^2)}{m_0^2}\frac{m_0^2}{(Q^2+m_0^2)}\right)}{\ln\frac{\Lambda^2_{sat}(W^2)}{m_0^2}} = 1 + \lim_{\substack{W^2\to\infty \\ Q^2 \text{ fixed}}} \frac{\ln\frac{m_0^2}{Q^2+m_0^2}}{\ln\frac{\Lambda^2_{sat}(W^2)}{m_0^2}} = 1.$$

$$\sigma_{\gamma^* p}\left(\eta(W^2,Q^2=0)\right) = \sigma_{\gamma p}(W^2)$$

D. Schildknecht, DIS 2001 (Bologna)

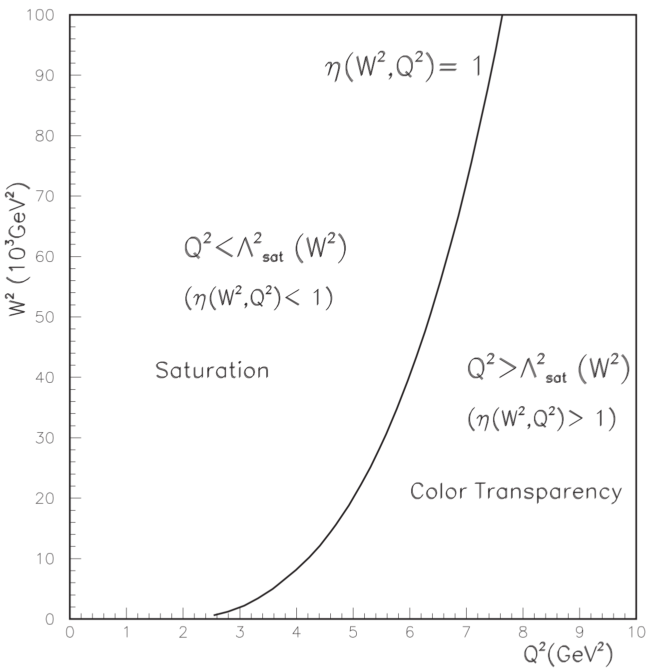

$Q^2[GeV^2]$	$W^2[GeV^2]$	$\frac{\sigma_{\gamma^* p}(\eta(W^2,Q^2))}{\sigma_{\gamma p}(W^2)}$
1.5	2.5×10^7	**0.5**
	1.26×10^{11}	**0.63**

Aim of the present talk

- Low-x scaling of $\sigma_{\gamma^* p}(\eta(W^2, Q^2))$,

- $\Lambda^2_{sat} \sim (W^2)^{C_2}, \qquad C_2 = 0.29 \qquad$ (DGLAP evolution),

- $F_L(x, Q^2) = 0.27 F_2(x, Q^2), \quad (Q^2 > \Lambda^2_{sat}(W^2))$

consequence of the interaction of

$q\bar{q}$ **color-dipole fluctuations of the photon with the proton.**

- Connection with gluon-distribution function and perturbative (DGLAP) evolution.
- No evidence for parton recombination and non-linear saturation in DIS.

2. Photon-hadron interactions: Late 1960's, early 1970's.

1960's Vector Meson Dominance

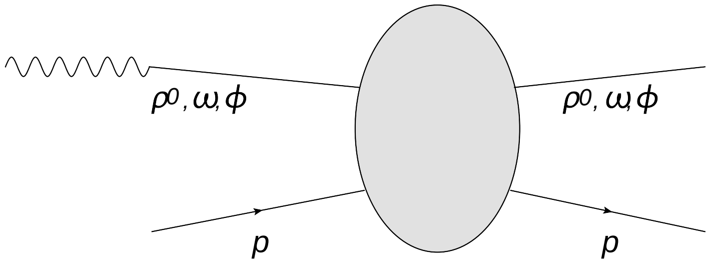

J.J. Sakurai (1960, ...)

Shadowing in γA interactions

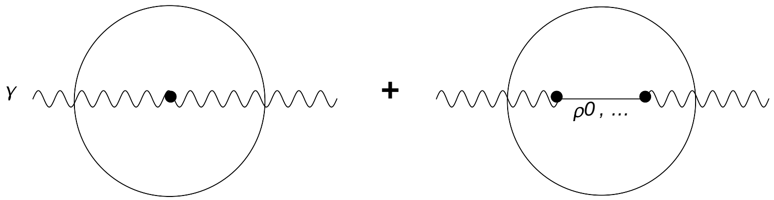

Leo Stodolsky (1967)

1969 DIS SLAC-MIT Collaboration

Bjorken scaling,

Feynman,parton model

(1972)

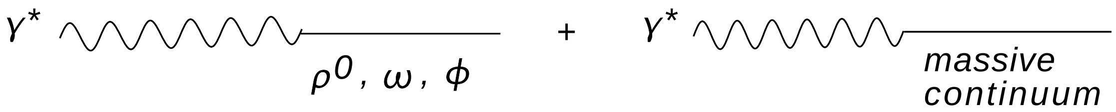

Volume 40B, number 1 PHYSICS LETTERS 12 June 1972

GENERALIZED VECTOR DOMINANCE AND INELASTIC ELECTRON-PROTON SCATTERING *

J. J. SAKURAI and D. SCHILDKNECHT **

Department of Physics, University of California, Los Angeles, USA

Received 30 March 1972

We propose a model of inelastic electron-proton scattering which takes into account the coupling of the photon to higher-mass vector states. Both the virtual photon-proton cross section σ_T (predicted with essentially no adjustable parameters) and the q^2 dependence of R are in exceedingly good agreement with the SLAC-MIT data in the diffraction region.

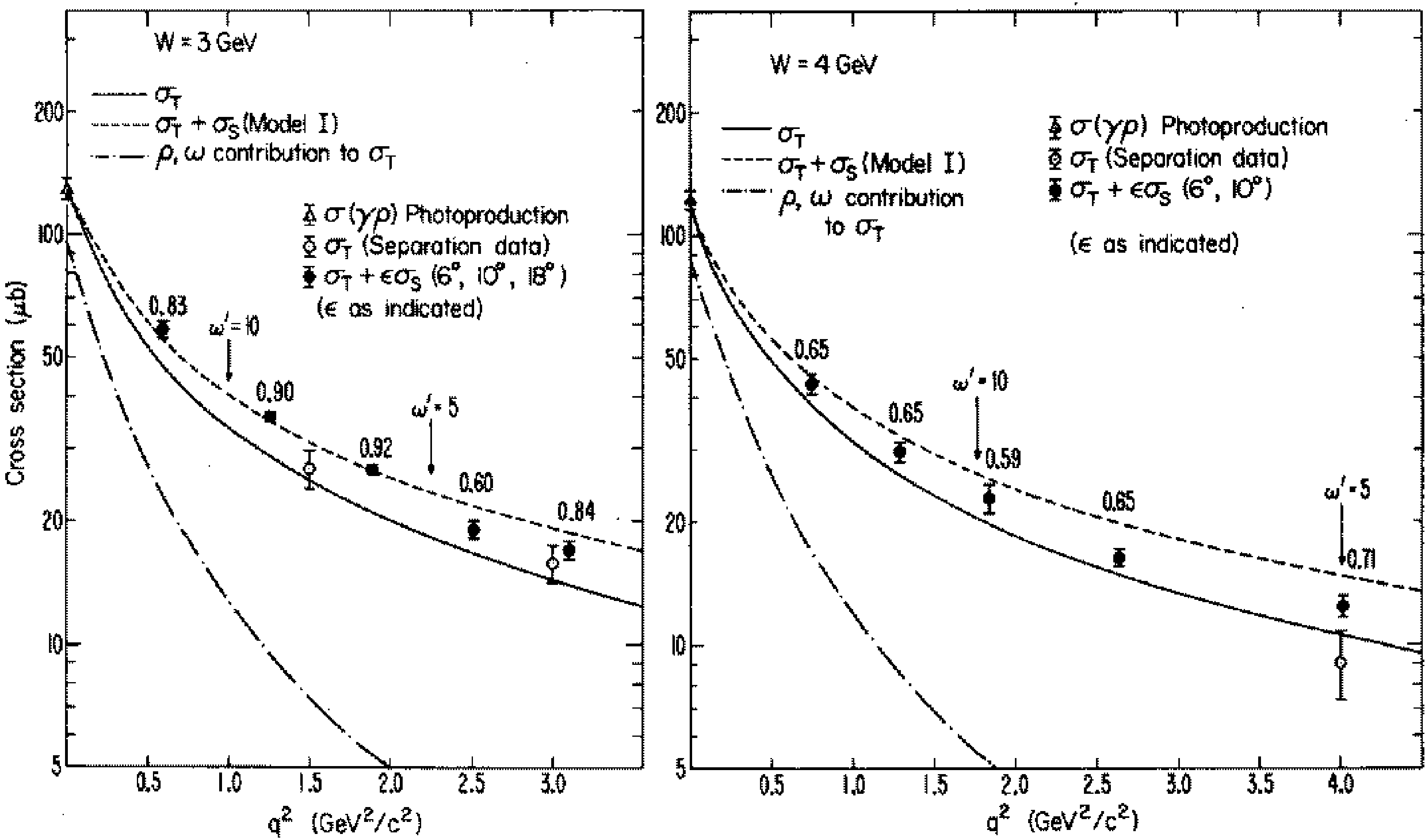

W = 3 GeV
σ_T
$\sigma_T + \sigma_S$ (Model I)
ρ, ω contribution to σ_T
$\sigma(\gamma p)$ Photoproduction
σ_T (Separation data)
$\sigma_T + \epsilon\sigma_S$ (6°, 10°, 18°)
(ϵ as indicated)
0.83
$\omega' = 10$
0.90
0.92
$\omega' = 5$
0.60
0.84
Cross section (μb)
q^2 (GeV^2/c^2)
W = 4 GeV
σ_T
$\sigma_T + \sigma_S$ (Model I)
ρ, ω contribution to σ_T
$\sigma(\gamma p)$ Photoproduction
σ_T (Separation data)
$\sigma_T + \epsilon\sigma_S$ (6°, 10°)
(ϵ as indicated)
0.65
0.65
$\omega' = 10$
0.59
0.65
$\omega' = 5$
0.71
q^2 (GeV^2/c^2)

1989 Shadowing EMC Collaboration

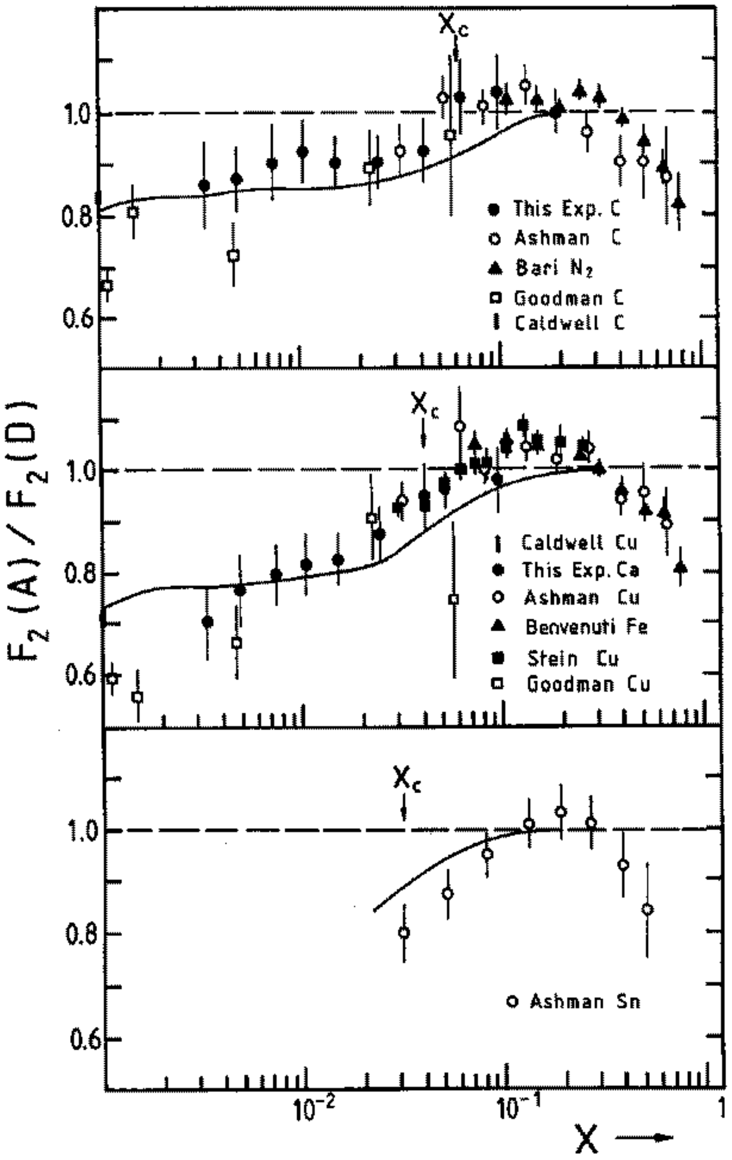

D. Schildknecht (1973)

C. Bilchak and D. Schildknecht (1989)

1994 HERA

DIS for $x_{bj} \ll 0.1$

High-mass diffractive production

("rap-gap"events).

Life time of hadronic fluctuations $\gamma^* \rightarrow \rho^0, \quad \gamma^* \rightarrow q\bar{q}$

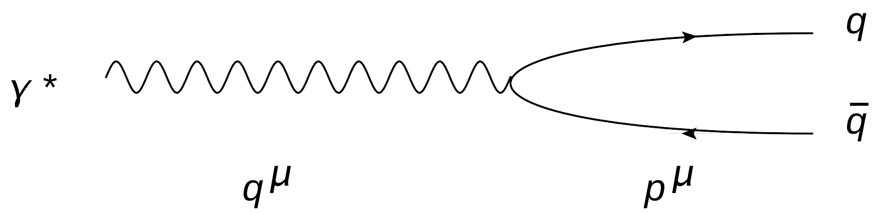

i) Four-momentum-conserving transition to virtual state, e.g. ρ^0, $q\bar{q}$ state

$$p^\mu = q^\mu,$$

$$p^2 = q^2 < 0, \qquad\qquad p^2 \neq M^2_{q\bar{q}},$$

Propagator: $\frac{1}{-q^2+M^2_{q\bar{q}}} = \frac{1}{Q^2+M^2_{q\bar{q}}}.$

ii) Equivalently: Three-momentum-conserving transition to on-shell $q\bar{q}$ state

$$\vec{p} = \vec{q};$$

$$p^2 = M_{q\bar{q}}^2; \quad q^2 = (q^0)^2 - (\vec{q})^2 < 0; \quad Q^2 = -q^2;$$

$$\Delta E = p^0 - q^0 = \frac{M_{q\bar{q}}^2 + Q^2}{p^0 + q^0}$$

$$\cong \frac{M_{q\bar{q}}^2 + Q^2}{2q^0}.$$

$$\tau = \frac{1}{\Delta E} = \frac{2M_p\nu}{Q^2 + M_{q\bar{q}}^2} \frac{1}{M_p} \gg \frac{1}{M_p}.$$

$(q\bar{q})p$ interaction cross section dependent on W (Q^2 and x dependence excluded).

Modern picture of low-x DIS:

i) $q\bar{q}$ internal structure

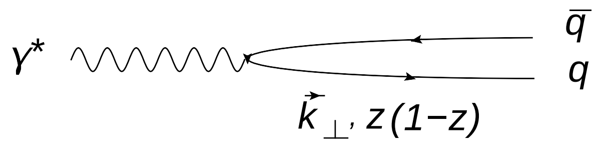

Nikolaev, Zakharov (1991)

ii) $q\bar{q}$-dipole interaction

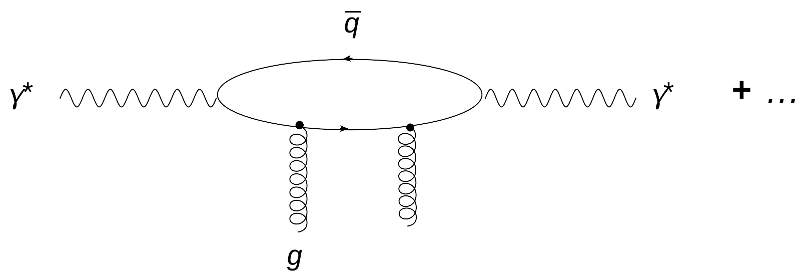

Low (1975)

Nussinov (1975)

Invariant mass of $q\bar{q}$ state

$$k^2 = k'^2 = m_q^2 = 0$$

$$\begin{aligned} M_{q\bar{q}}^2 &= (k + k')^2 = (2k^0_{C.M.})^2 \\ &= 4\frac{\vec{k}_\perp^{\,2}}{\sin^2\vartheta_{C.M.}} \end{aligned}$$

In terms of z: $\quad 0 \leq z \leq 1$

$$k^3 = zq^3;$$

$$k'^3 = (1 - z)q^3;$$

$$M_{q\bar{q}}^2 = \frac{\vec{k}_\perp^{\,2}}{z(1-z)};$$

$$\sin^2\vartheta_{C.M.} = 4z(1 - z)$$

3. The Color Dipole Picture (CDP).

The longitudinal and the transverse photoabsorption cross section

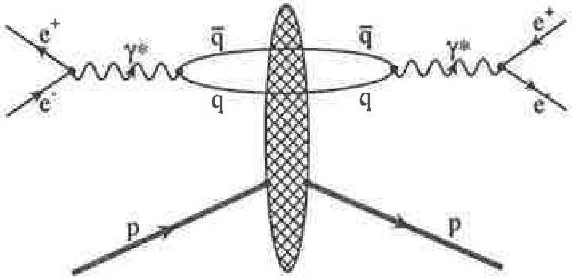

(a)

channel 1:

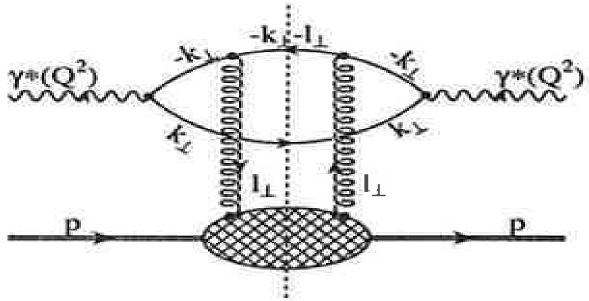

(a)

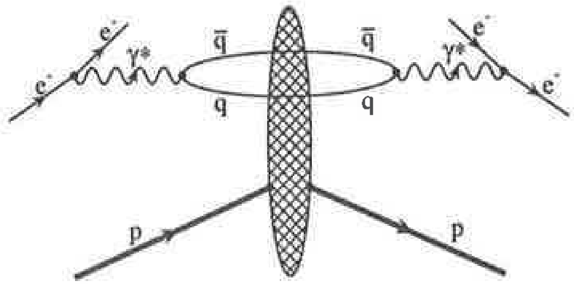

(b)

channel 2:

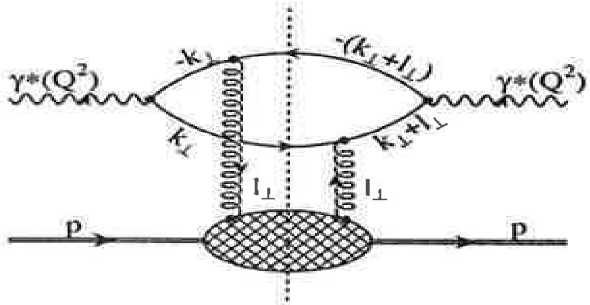

(b)

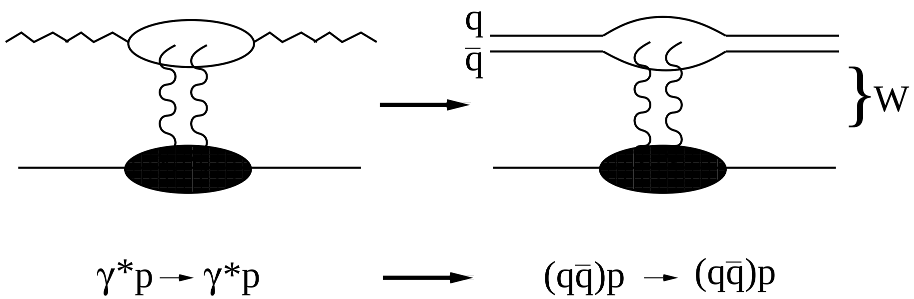

A) $$\sigma_{\gamma^*_{L,T}}(W^2, Q^2) = \int dz \int d^2\vec{r}_\perp |\psi_{L,T}(\vec{r}_\perp, z(1-z), Q^2)|^2 \;\; \sigma_{(q\bar{q})p}(\vec{r}_\perp, z(1-z), W^2)$$

Remarks: i) $|\psi_{L,T}(\vec{r}_\perp, z(1-z), Q^2)|$: Probability for $\gamma^*_{L,T} \to q\bar{q}$ fluctuation

ii) $\sigma_{(q\bar{q})p}(\vec{r}_\perp, z(1-z), W^2)$: $(q\bar{q})p$ cross section dependent on W^2 (not on $x \equiv \frac{Q^2}{W^2}$)

B) Gauge-invariant two-gluon coupling:

$$\sigma_{(q\bar{q})p}(\vec{r}_\perp, z(1-z), W^2) = \int d^2\vec{l}_\perp \tilde{\sigma}(\vec{l}_\perp^{\,2}, z(1-z), W^2) \left(1 - e^{-i\, \vec{l}_\perp \cdot \vec{r}_\perp}\right)$$

Nikolaev, Zakharov (1991)

Cvetic, Schildknecht, Shoshi(2000)

Equivalently, in terms of the variables:

$$\vec{r}_\perp{}' = \sqrt{z(1-z)}\,\vec{r}_\perp,$$

$$\vec{l}_\perp{}' = \frac{\vec{l}_\perp}{\sqrt{z(1-z)}},$$

Photon wave function (e.g. L):

$$K_0(r'_\perp Q) = \frac{1}{2\pi}\int d^2\vec{k}_\perp{}' \frac{1}{Q^2 + \vec{k}_\perp{}'^2} e^{-i\vec{r}_\perp{}' \cdot \vec{k}_\perp{}'}$$

$\gamma^* q\bar{q}$ **coupling :** $$\sum_{\lambda=-\lambda=\pm 1} |j_L^{\lambda,\lambda'}|^2 = 4M_{q\bar{q}}^2 \left(d_{10}^1(z)\right)^2,$$

$$\sum_{\lambda=-\lambda'=\pm 1} |j_T^{\lambda,\lambda'}(+)|^2 = \sum_{\lambda=-\lambda=\pm 1} |j_T^{\lambda,\lambda'}(-)|^2 = 4M_{q\bar{q}}^2 \frac{1}{2}\left((d_{1-1}^1(z))^2 + (d_{11}^1(z))^2\right).$$

Upon introducing the cross section $\sigma_{(q\bar{q})^{J=1}_{L,T}p}(r'_\perp, W^2)$, for $(q\bar{q})^{J=1}_{L,T}p$ scattering

A) $\sigma_{\gamma^*_{L,T}p}(W^2, Q^2) = \frac{\alpha}{\pi}\sum_q Q_q^2 Q^2 \int dr'^2_\perp K^2_{0,1}(r'_\perp Q)\sigma_{(q\bar{q})^{J=1}_{L,T}p}(r'_\perp, W^2).$ Kuroda, Schildknecht (2011)

and

B)
$$\begin{aligned}\sigma_{(q\bar{q})^{J=1}_{L,T}p}(\vec{r}_\perp{}', W^2) &= \int d^2\vec{l}_\perp{}' \bar{\sigma}_{(q\bar{q})^{J=1}_{L,T}p}(\vec{l}_\perp{}'^2, W^2)(1 - e^{-i\vec{l}_\perp{}'\cdot\vec{r}_\perp{}'}) \\ &= \pi \int d\vec{l}_\perp{}'^2 \bar{\sigma}_{(q\bar{q})^{J=1}_{L,T}p}(\vec{l}_\perp{}'^2, W^2)\cdot\left(1 - \frac{\int d\vec{l}_\perp{}'^2 \bar{\sigma}_{(q\bar{q})^{J=1}_{L,T}p}(\vec{l}_\perp{}'^2, W^2) J_0(l'_\perp r'_\perp)}{\int d\vec{l}_\perp{}'^2 \bar{\sigma}_{(q\bar{q})^{J=1}_{L,T}p}(\vec{l}_\perp{}'^2, W^2)}\right)\end{aligned}$$

For fixed dipole size, $r'_\perp$, dominant contribution to dipole cross section

$$\vec{l}_\perp{}'^2 \leq \vec{l}_{\perp \mathrm{Max}}'^2(W^2).$$

The Color Dipole Cross Section.

I) Color transparency

$$0 < l'_\perp r'_\perp < l'_{\perp\ Max}(W^2) r'_\perp \ll 1, \qquad\qquad J_0(l'_\perp r'_\perp) \cong 1 - \frac{1}{4}(l'_\perp r'_\perp)^2$$

$$\sigma_{(q\bar{q})^{J=1}_{L,T}p}(r'^2_\perp, W^2) =$$
$$= \frac{1}{4}\pi r'^2_\perp \int d\vec{l}'^2_\perp \vec{l}'^2_\perp \bar{\sigma}_{(q\bar{q})^{J=1}_L p}(\vec{l}'^2_\perp, W^2) \begin{cases} 1, \\ \rho_W, \end{cases} \qquad \left(r'^2_\perp \ll \frac{1}{l'^2_{\perp\ Max}(W^2)} \right).$$

where $\int d\vec{l}'^2_\perp \vec{l}'^2_\perp \bar{\sigma}_{(q\bar{q})^{J=1}_T p}(\vec{l}'^2_\perp, W^2) = \rho_W \int d\vec{l}'^2_\perp \vec{l}'^2_\perp \bar{\sigma}_{(q\bar{q})^{J=1}_L p}(\vec{l}'^2_\perp, W^2)$.

$$\sigma_{(q\bar{q})^{J=1}_{L,T}p}(r'^2_\perp, W^2) = \frac{1}{4} r'^2_\perp \sigma^{(\infty)}_L(W^2) \Lambda^2_{sat}(W^2) \begin{cases} 1, \\ \rho_W, \end{cases} \qquad \left(r'^2_\perp \ll \frac{1}{l'^2_{\perp\ Max}(W^2)} \right).$$

where $\Lambda^2_{sat}(W^2) \equiv \frac{\int d\vec{l}'^2_\perp \vec{l}'^2_\perp \bar{\sigma}_{(q\bar{q})^{J=1}_L p}(\vec{l}'^2_\perp, W^2)}{\int d\vec{l}'^2_\perp \bar{\sigma}_{(q\bar{q})^{J=1}_L p}(\vec{l}'^2_\perp, W^2)}$

Strong cancellation between channel 1 and channel 2.

II) Saturation

$l'_{\perp Max}(W^2) r'_\perp \gg 1,$

huge integrations range in integral over $dl'^2_\perp$, many oscillations of $J_0(l'_\perp r'_\perp)$, contribution from channel 2 vanishing

$$\sigma_{(q\bar{q})^{J=1}_{L,T} p}(r'^2_\perp, W^2) \quad \cong \pi \int d\vec{l}'^2_\perp \bar{\sigma}_{(q\bar{q})^{J=1}_{L,T} p}(\vec{l}'^2_\perp, W^2) \equiv \sigma^{(\infty)}_{L,T}(W^2),$$
$$\left(r'^2_\perp \gg \frac{1}{l'^2_{\perp \; Max}(W^2)} \right).$$

Unitarity: $\sigma^{(\infty)}_{L,T}(W^2)$ at most logarithmically dependent on W^2.

Thus: Property of dipole interaction:

$$\lim_{\substack{r'^2_\perp \text{fixed} \\ W^2 \to \infty}} \sigma_{(q\bar{q})^{J=1}_{L,T} p}(r'_\perp, W^2) = \lim_{\substack{r'^2_\perp \to \infty \\ W^2 \text{fixed}}} \sigma_{(q\bar{q})^{J=1}_{L,T} p}(r'^2_\perp, W^2)$$

Photoabsorption Cross Section

Due to $K_{0,1}^2(r'_\perp Q) \sim \frac{\pi}{2r'_\perp Q} e^{-2r'_\perp Q}$, $\quad (r'_\perp Q \gg 1)$, cross section determined by

$$r'^2_\perp < \frac{1}{Q^2}.$$

At fixed Q^2,

either $\; r'^2_\perp < \frac{1}{Q^2} < \frac{1}{\Lambda^2_{sat}(W^2)}$, color transparency: $Q^2 \gg \Lambda^2_{sat}(W^2)$

or $\; \frac{1}{\Lambda^2_{sat}(W^2)} < r'^2_\perp < \frac{1}{Q^2}$, saturation: $\Lambda^2_{sat}(W^2) \gg Q^2$.

$$\begin{aligned}\sigma_{\gamma^* p}(W^2, Q^2) &= \sigma_{\gamma^* p}(\eta(W^2, Q^2)) = \\ &= \frac{\alpha}{\pi} \sum_q Q_q^2 \begin{cases} \sigma_T^{(\infty)}(W^2) \ln \frac{1}{\eta(W^2,Q^2)}, & (\eta(W^2, Q^2) \ll 1) \qquad \text{(sat.)}, \\ \frac{1}{6}(1+2\rho)\sigma_L^{(\infty)}(W^2) \frac{1}{\eta(W^2,Q^2)}, & (\eta(W^2, Q^2) \gg 1), \quad \text{(col.tr.)} \end{cases}\end{aligned}$$

$$\eta(W^2, Q^2) = \frac{Q^2 + m_0^2}{\Lambda^2_{sat}(W^2)}$$

Color-gauge-invariant $q\bar{q}$ (dipole) interaction with gluon field in the nucleon implies low-x scaling.

Low-x Scaling

Empirically : $\eta(W^2, Q^2) \equiv \dfrac{Q^2 + m_0^2}{\Lambda^2_{sat}(W^2)}$,

$$\Lambda^2_{sat}(W^2) \sim (W^2)^{C_2}$$

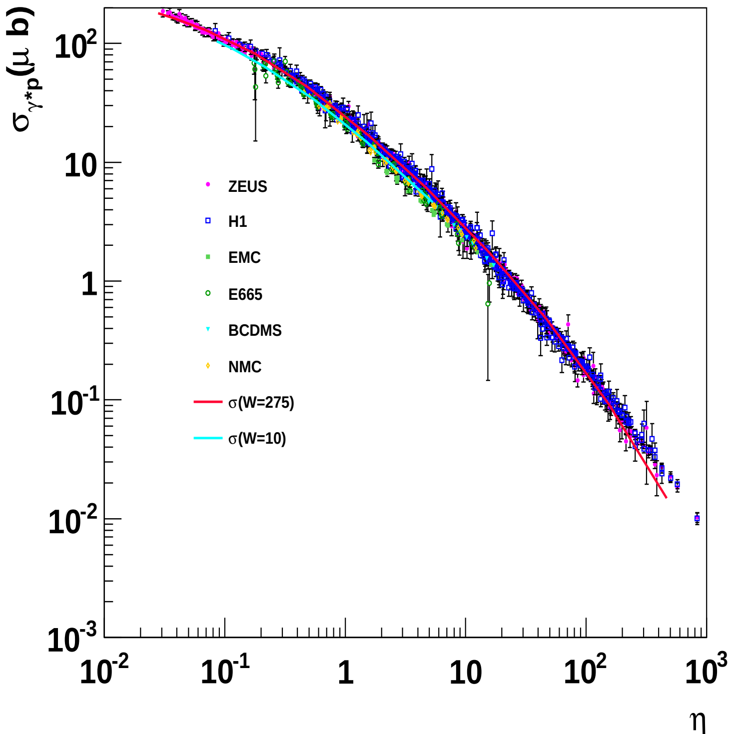

Schildknecht, Surrow, Tentyukov (2000)

$$\begin{aligned}\sigma_{\gamma^*p}(W^2, Q^2) &= \sigma_{\gamma^*p}(\eta(W^2, Q^2)) \\ &\sim \sigma^{(\infty)} \begin{cases} ln\frac{1}{\eta(W^2,Q^2)} & , \quad \text{for } \eta(W^2, Q^2) \ll 1 \\ \frac{1}{\eta(W^2,Q^2)} & , \quad \text{for } \eta(W^2, Q^2) \gg 1 \end{cases}\end{aligned}$$

The W-dependence

$$
\begin{aligned}
F_2(x,Q^2) &\cong \frac{Q^2}{4\pi^2\alpha}\left(\sigma_{\gamma_L^* p}(W^2,Q^2)+\sigma_{\gamma_T^* p}(W^2,Q^2)\right)\\
&= \frac{\sum_q Q_q^2}{4\pi^2}\int dz \int d\vec{l}_\perp^{\,2}\vec{l}_\perp^{\,2}\tilde{\sigma}(\vec{l}_\perp^{\,2}, z(1-z), W^2)(1+2\rho)\\
&= F_2(W^2)\ \ \text{for}\ \ x<0.1.
\end{aligned}
$$

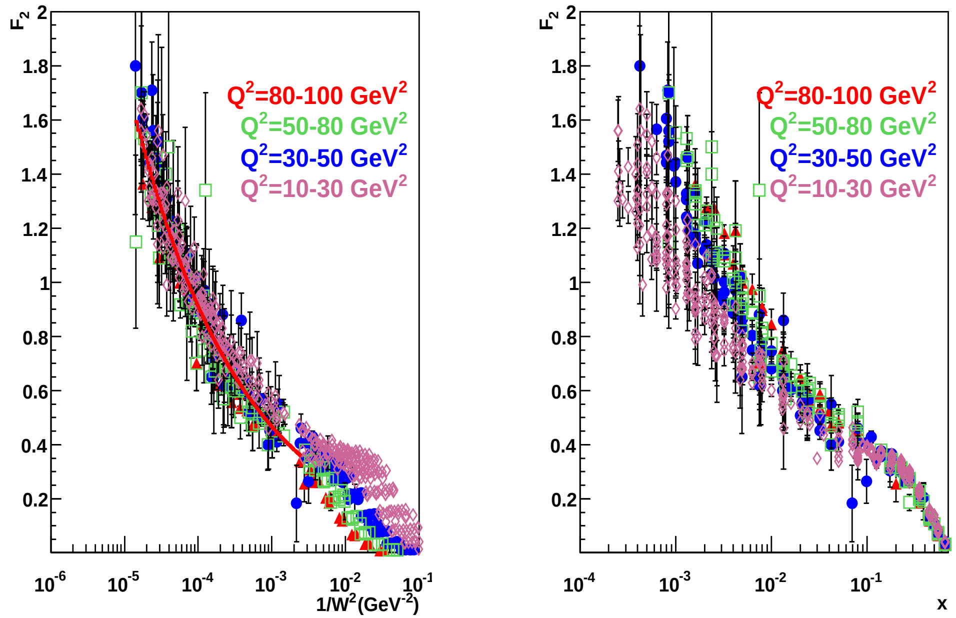

Prabhdeep Kaur (2010)

The limit of $\eta(W^2, Q^2) \to 0$, or $W^2 \to \infty$ at Q^2 fixed

$$\lim_{\substack{W^2\to\infty \\ Q^2 \text{ fixed}}} \frac{\sigma_{\gamma^* p}(\eta(W^2,Q^2))}{\sigma_{\gamma^* p}(\eta(W^2,Q^2=0))} = \lim_{\substack{W^2\to\infty \\ Q^2 \text{ fixed}}} \frac{\ln\left(\frac{\Lambda^2_{sat}(W^2)}{m_0^2}\frac{m_0^2}{(Q^2+m_0^2)}\right)}{\ln\frac{\Lambda^2_{sat}(W^2)}{m_0^2}} = 1 + \lim_{\substack{W^2\to\infty \\ Q^2 \text{ fixed}}} \frac{\ln\frac{m_0^2}{Q^2+m_0^2}}{\ln\frac{\Lambda^2_{sat}(W^2)}{m_0^2}} = 1.$$

$$\sigma_{\gamma^* p}\left(\eta(W^2,Q^2=0)\right) = \sigma_{\gamma p}(W^2)$$

D. Schildknecht, DIS 2001 (Bologna)

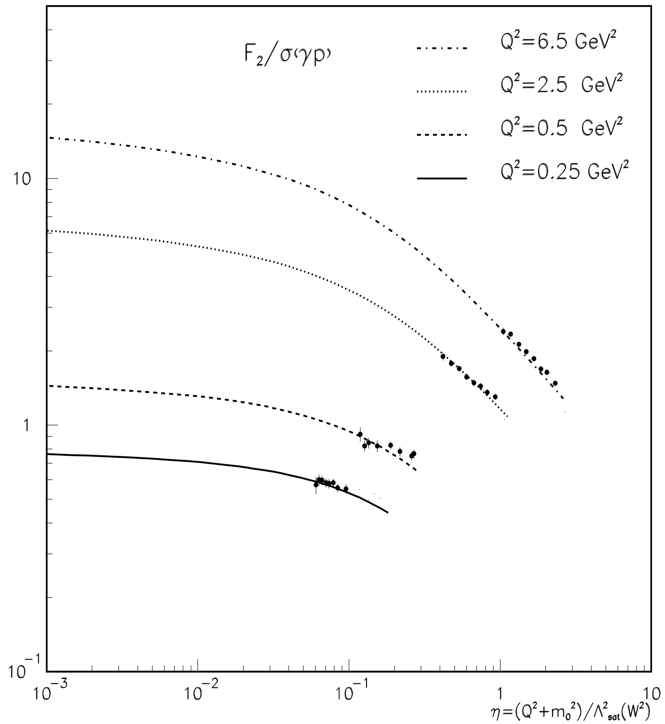

$$\lim_{\substack{W^2\to\infty \\ Q^2 \text{fixed}}} \frac{F_2(x\cong Q^2/W^2, Q^2)}{\sigma_{\gamma p}(W^2)} = \frac{Q^2}{4\pi^2\alpha}.$$

$Q^2[GeV^2]$	$W^2[GeV^2]$	$\frac{\sigma_{\gamma^* p}(\eta(W^2,Q^2))}{\sigma_{\gamma p}(W^2)}$
1.5	2.5×10^7	**0.5**
	1.26×10^{11}	**0.63**

Observation by Caldwell

$$\sigma_{\gamma^* p}(W^2, Q^2) = \sigma_0(Q^2)\left(\frac{1}{2}\frac{W^2}{Q^2}\right)^{\lambda_{eff}(Q^2)} \equiv \sigma_0(Q^2) l^{\lambda_{eff}(Q^2)}$$

A. Caldwell (2008)

Q^2-independent limit at approximately

$$W^2 \simeq 10^9 Q^2.$$

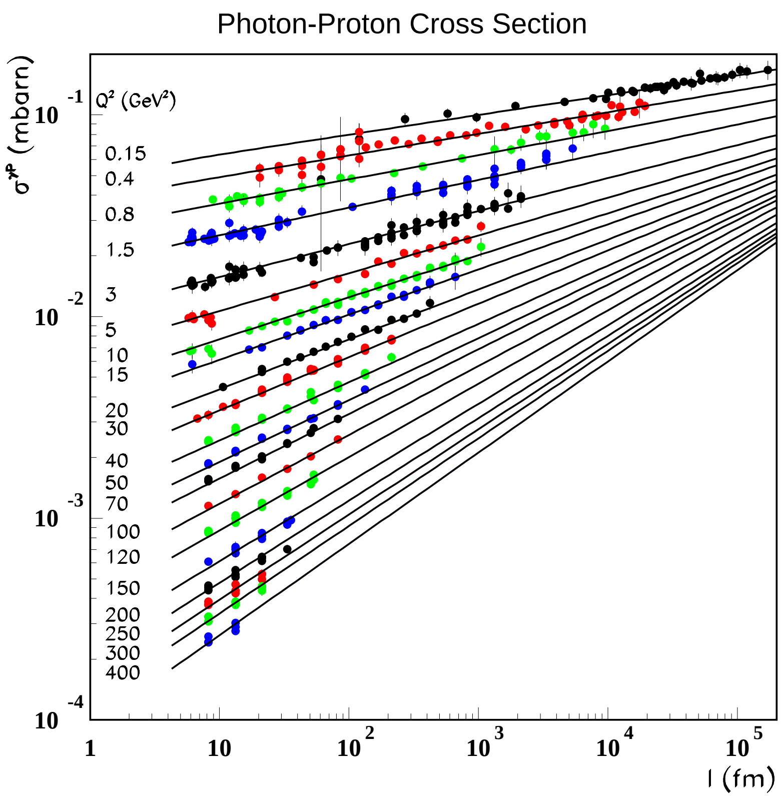

The (Q^2, W^2) plane

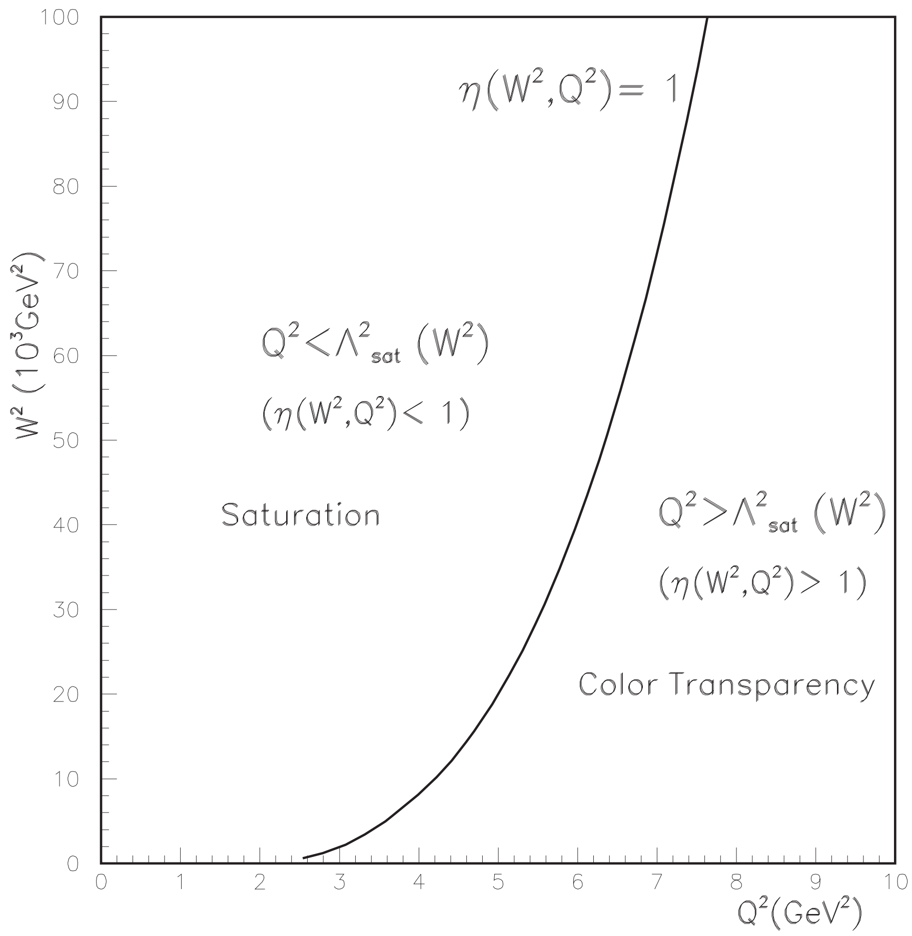

The longitudinal-to-transverse ratio

$(q\bar{q})^{J=1}_{L,T}$ states : $\gamma^*_{L,T} \to (q\bar{q})^{J=1}_{L,T}$

$$\sigma_{\gamma^*_{L,T}p}(W^2, Q^2) = \alpha \sum_q Q_q^2 \frac{1}{Q^2} \frac{1}{6} \begin{cases} \int d\vec{l}_\perp'^2 \vec{l}_\perp'^2 \bar{\sigma}_{(q\bar{q})^{J=1}_L p}(\vec{l}_\perp'^2, W^2), \\ 2 \int d\vec{l}_\perp'^2 \vec{l}_\perp'^2 \bar{\sigma}_{(q\bar{q})^{J=1}_T p}(\vec{l}_\perp'^2, W^2). \end{cases}$$

$$\rho_W = \frac{\int d\vec{l}_\perp'^2 \vec{l}_\perp'^2 \bar{\sigma}_{(q\bar{q})^{J=1}_T p}(\vec{l}_\perp'^2, W^2)}{\int d\vec{l}_\perp'^2 \vec{l}_\perp'^2 \bar{\sigma}_{(q\bar{q})^{J=1}_L p}(\vec{l}_\perp'^2, W^2)}.$$

Numerical value of $\rho_W = \rho$:

$\vec{l}_\perp^{\,2} = z(1-z)\vec{l}_\perp'^2$

$$\langle \vec{l}_\perp^{\,2} \rangle_{L,T}^{\vec{l}_\perp'^2 = const} = \vec{l}_\perp'^2 \begin{cases} 6 \int dz z^2 (1-z)^2 = \frac{4}{20} \vec{l}_\perp'^2, \\ \frac{3}{2} \int dz \; z(1-z)(1-2z(1-z)) = \frac{3}{20} \vec{l}_\perp'^2. \end{cases}$$

Uncertainty principle:

$$\rho_W = \frac{\langle r_\perp^2 \rangle_T}{\langle \vec{r}_\perp^{\,2} \rangle_L} = \frac{\langle \vec{l}_\perp^{\,2} \rangle_L}{\langle \vec{l}_\perp^{\,2} \rangle_T} = \frac{4}{3} \equiv \rho.$$

$$R = \frac{1}{2\rho} = \begin{cases} 0.5 \text{ for } \rho = 1, \\ \frac{3}{8} = 0.375 \text{ for } \rho = \frac{4}{3}. \end{cases}$$

ad hoc, helicity independence

Kuroda, Schildknecht (2008)

For $\rho = \frac{4}{3}$: $F_L = 0.27 F_2$

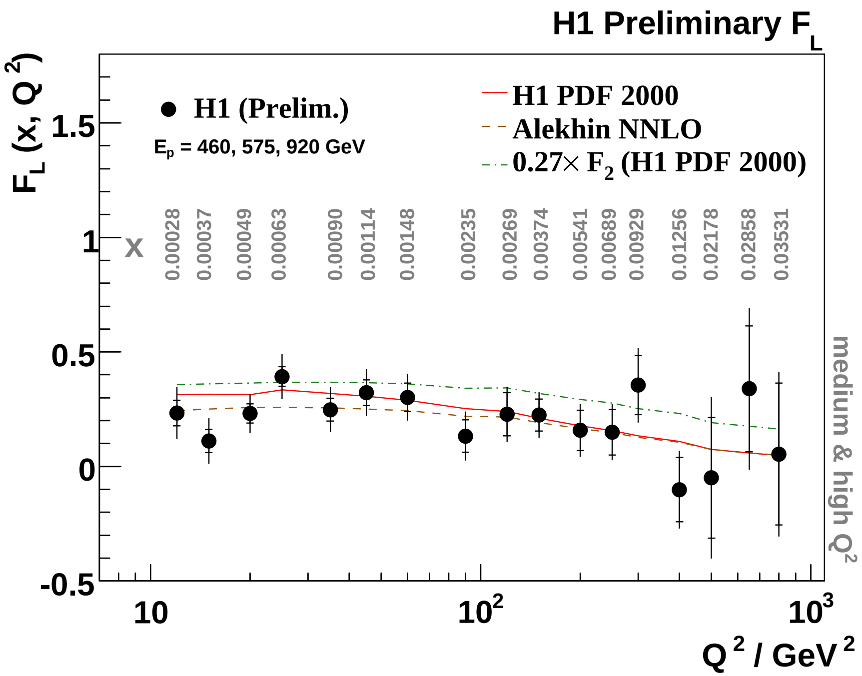

H1 Preliminary F_L
H1 (Prelim.)
E_p = 460, 575, 920 GeV
H1 PDF 2000
Alekhin NNLO
0.27× F_2 (H1 PDF 2000)
F_L (x, Q^2)
Q^2 / GeV^2
medium & high Q^2
x
0.00028
0.00037
0.00049
0.00063
0.00090
0.00114
0.00148
0.00235
0.00269
0.00374
0.00541
0.00689
0.00929
0.01256
0.02178
0.02858
0.03531

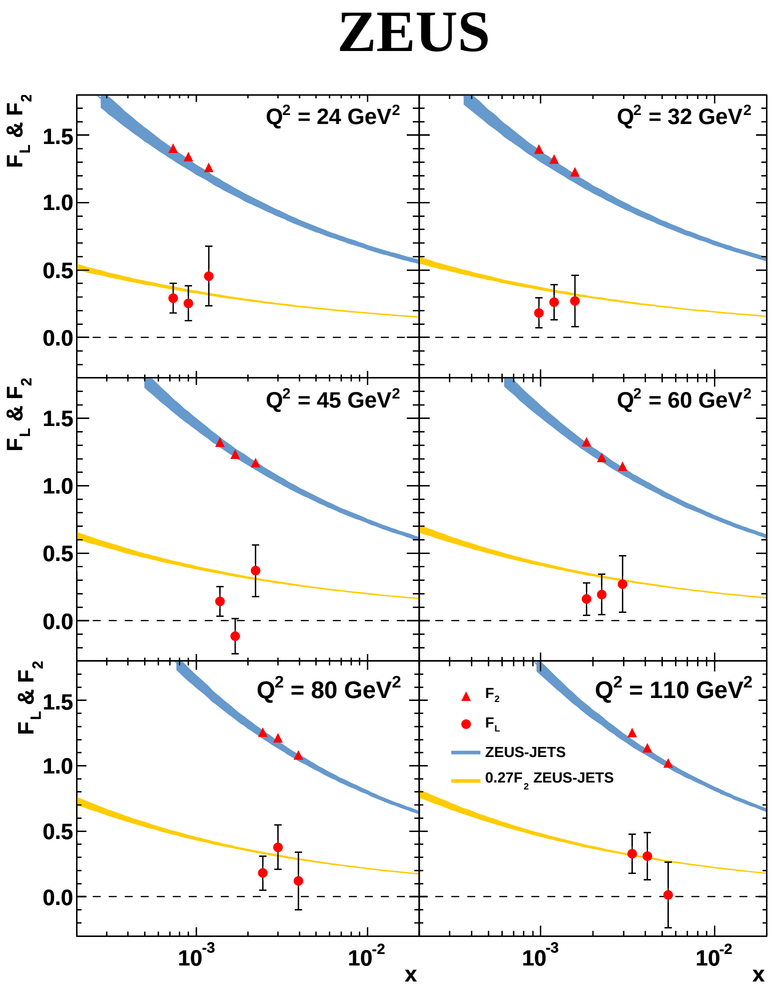

ZEUS
Q^2 = 24 GeV^2
Q^2 = 32 GeV^2
Q^2 = 45 GeV^2
Q^2 = 60 GeV^2
Q^2 = 80 GeV^2
Q^2 = 110 GeV^2
F_L & F_2
F_2
F_L
ZEUS-JETS
0.27F_2 ZEUS-JETS
x

Ewerz et al., arXiv: 1201.6296

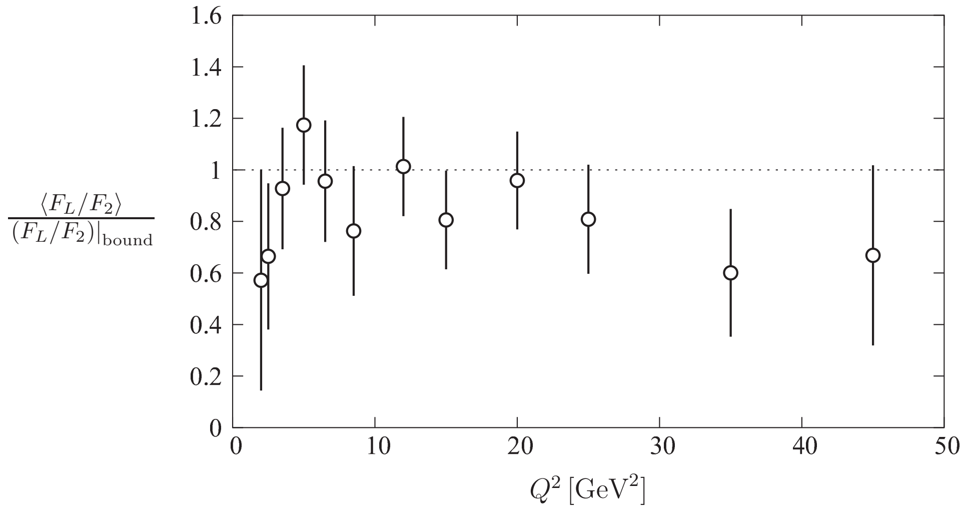

$$\frac{(F_L/F_2)}{(F_L/F_2)|_{bound}} = \frac{(F_L/F_2)}{0.27} \simeq 1$$

4. The CDP, the Gluon Distribution Function and Evolution.

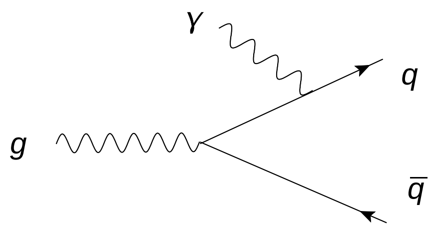

CDP $\leftrightarrow$ Photon-Gluon Fusion of pQCD

$F_L(x,Q^2) = \frac{\alpha_s(Q^2)}{3\pi}\sum_q Q_q^2 \cdot 6 I_g(x,Q^2),$

where $I_g(x,Q^2) \equiv \int_x^1 \frac{dy}{y}\left(\frac{x}{y}\right)^2\left(1-\frac{x}{y}\right) yg(y,Q^2).$

$F_L(\xi_L x, Q^2) = \frac{\alpha_s(Q^2)}{3\pi}\sum_q Q_q^2 G(x,Q^2).$ Cooper-Sarkar et al. (1988)

$F_2(x,Q^2) = \frac{5}{18} x \sum(x,Q^2).$

$\frac{\partial F_2(\xi_2 x, Q^2)}{\partial \ln Q^2} = \frac{\alpha_s(Q^2)}{3\pi}\sum_q Q_q^2 G(x,Q^2).$

rescaling factors:

$(\xi_L,\xi_2) \simeq (0.40, 0.50)$

$(\xi_L,\xi_2) = (0.45, 0.40)$ for specific gluon distribution. Prytz (1993)

Accuracy $\lesssim$0.5 %.

Using $F_L(x,Q^2) = \frac{1}{2\rho+1} F_2(x,Q^2)$:

$$(2\rho+1)\frac{\partial}{\partial \ln Q^2} F_2\left(\frac{\xi_2}{\xi_L}x, Q^2\right) = F_2(x,Q^2)$$

i) CDP: $F_2(x,Q^2) = F_2(W^2)$:

$$(2\rho_W+1)\frac{\partial}{\partial \ln W^2} F_2\left(\frac{\xi_L}{\xi_2}W^2\right) = F_2(W^2)$$

ii) Power law

$$F_2(W^2) \sim (W^2)^{C_2} = \left(\frac{Q^2}{x}\right)^{C_2}$$

Compare: "hard Pomeron" solution of DGLAP evolution: $\left(\frac{1}{x}\right)^{\lambda = \text{ fixed}}$.

"hard Pomeron" Regge: $\left(\frac{1}{x}\right)^{\epsilon_0 \simeq 0.43}$

$$(2\rho_W+1)C_2\left(\frac{\xi_L}{\xi_2}\right)^{C_2} = 1,$$

$\rho = \frac{4}{3}$: $\quad C_2 = \frac{1}{2\rho+1}\left(\frac{\xi_2}{\xi_L}\right)^{C_2} = 0.29$ Kuroda, Schildknecht (2005, 2011)

"BFKL-Pomeron": $\left(\frac{1}{x}\right)^{\lambda = \frac{12\alpha_s}{\pi}\ln 2}$

Balitskii, Fadin, Kuraev, Lipatov (1978/79)

$$F_2(W^2) = f_2 \cdot \left(\frac{W^2}{1\mathrm{GeV}^2}\right)^{C_2=0.29}$$

$$f_2 = 0.063 \quad \text{(fitted parameter)}$$

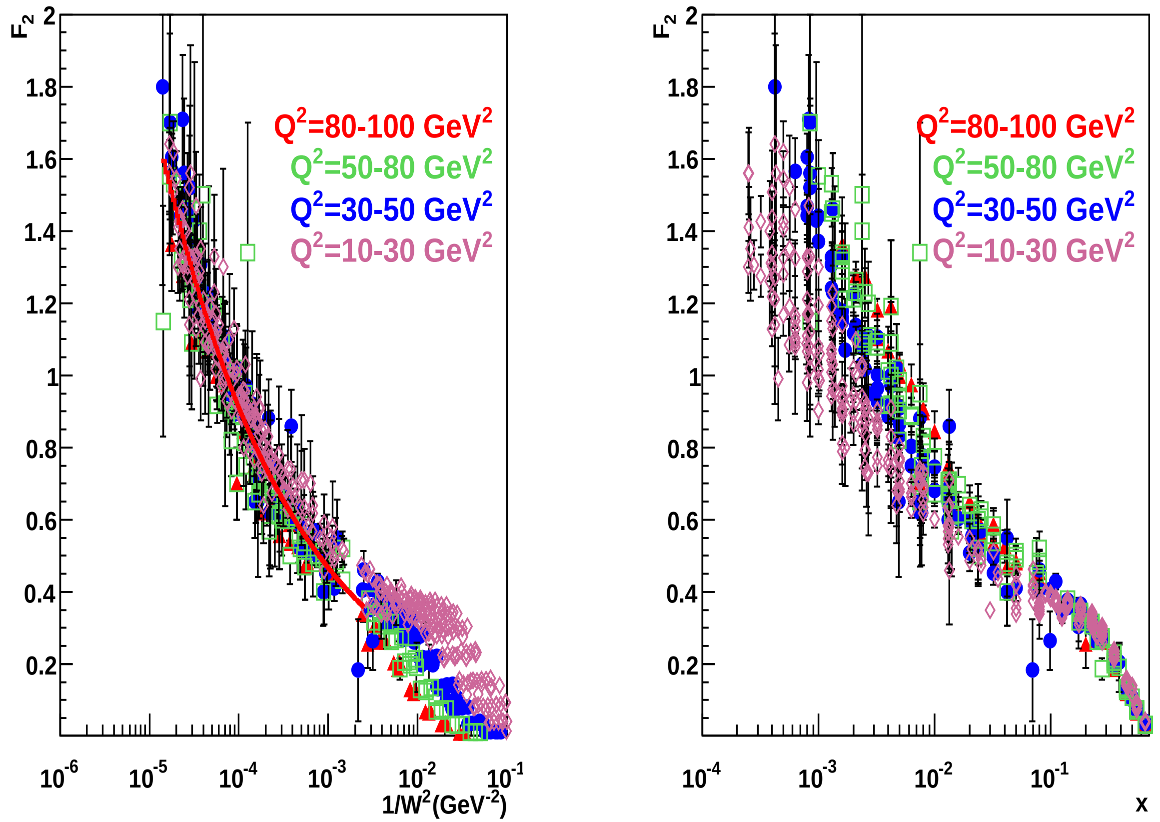

Experimental evidence for $F_2(x, Q^2) = F_2(W^2 \cong Q^2/x)$

and for the prediction of $C_2 = 0.29$.

The Gluon Distribution Function

$$
\begin{aligned}
\alpha_s(Q^2)G(x,Q^2) &= \frac{3\pi}{\sum_q Q_q^2} F_L(\xi_L x, Q^2) \\
&= \frac{3\pi}{\sum_q Q_q^2} \frac{1}{(2\rho+1)} F_2(\xi_L x, Q^2) \\
&= \frac{3\pi}{\sum_q Q_q^2 (2\rho+1)} \frac{f_2}{\xi_L^{C_2=0.29}} \left(\frac{W^2}{1\mathrm{GeV}^2}\right)^{C_2=0.29}
\end{aligned}
$$

Comments:

CDP: $F_{L,2} = F_{L,2}\left(W^2 = \frac{Q^2}{x}\right)$,

$\rho =$ const. $= \frac{4}{3}$,

$C_2 = 0.29$ from evolution

$f_2 = 0.063$ fit parameter

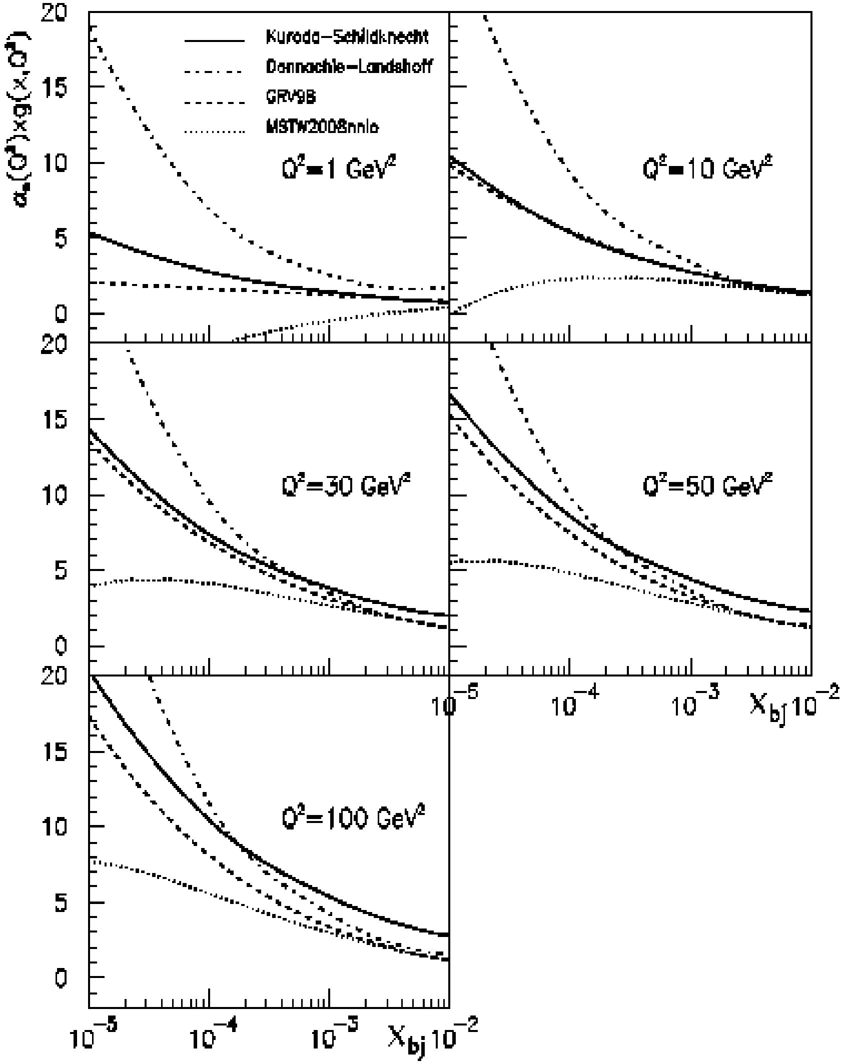

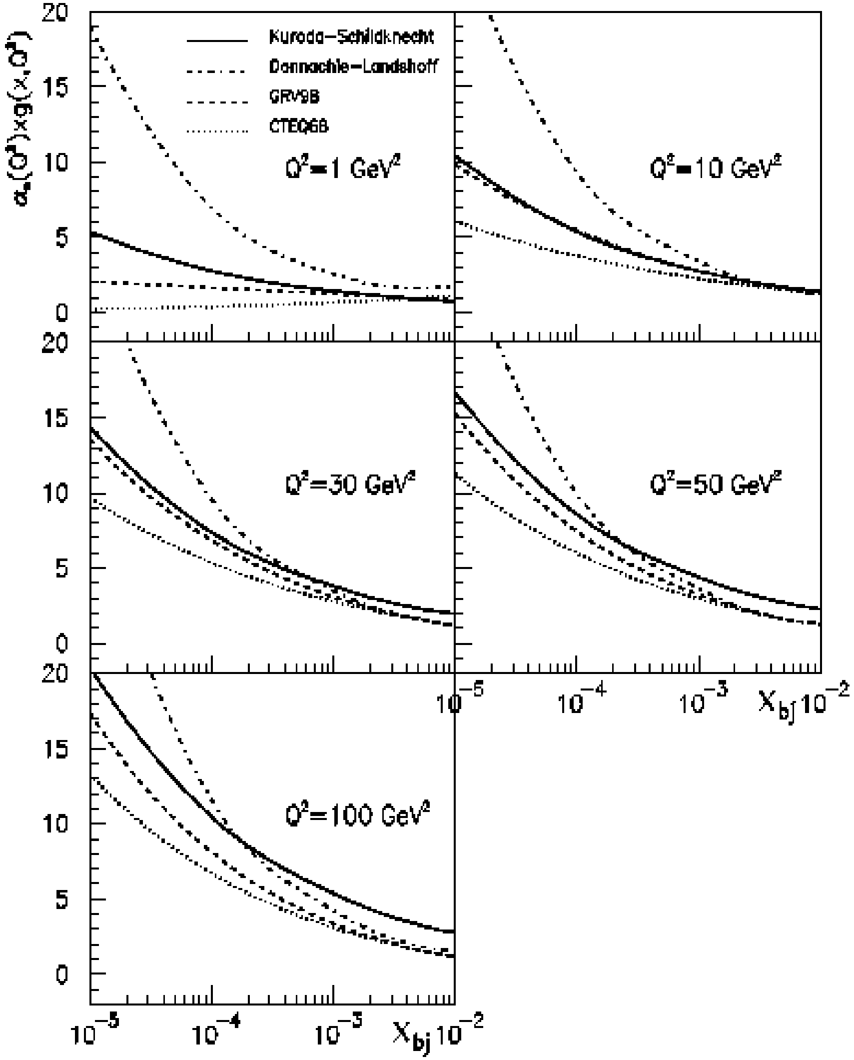

Comparison with gluon distributions from Durham data file using $\alpha_s(Q^2) = \alpha_s(Q^2)^{NLO}$

Inversion: $F_2(W^2)$ in terms of gluon distribution:

$$F_2\left(W^2=\frac{Q^2}{x}\right) = \frac{(2\rho+1)\sum Q_q^2}{3\pi}\xi_L^{C_2}\alpha_s(Q^2)G(x,Q^2) \qquad \eta(W^2,Q^2)\gg 1.$$

$$= \frac{(2\rho+1)\sum Q_q^2}{3\pi}\frac{1}{8\pi^2}\sigma_L^{(\infty)}\Lambda^2_{sat}(W^2). \qquad \text{color transparency}$$

(upon using $F_2 = f_2\left(\frac{W^2}{1GeV^2}\right)^{0.29} = \frac{(2\rho+1)\sum Q_q^2}{3\pi}\frac{1}{8\pi^2}\sigma_L^{(\infty)}\Lambda^2_{sat}(W^2)$.)

Saturation behavior:

$$F_2(W^2,Q^2) \sim Q^2\sigma_L^{(\infty)}\ln\frac{\Lambda^2_{\rm sat}(W^2)}{Q^2+m_0^2}$$

$$\sim Q^2\sigma_L^{(\infty)}\ln\left(\frac{\alpha_s(Q^2)G(x,Q^2)}{\sigma_L^{(\infty)}(Q^2+m_0^2)}\right), \qquad \eta(W^2,Q^2)\ll 1.$$

saturation

Logarithmic dependence on gluon distribution in saturation limit.

5. Model for the Dipole Cross Section

Model-independently:

$$\sigma_{\gamma^* p} \sim \begin{cases} ln \frac{1}{\eta(W^2,Q^2)} & , \quad \eta(W^2,Q^2) \ll 1 \\ \frac{1}{\eta(W^2,Q^2)} & , \quad \eta(W^2,Q^2) \gg 1 \end{cases}$$

Interpolation between $\eta(W^2,Q^2) < 1$ and $\eta(W^2,Q^2) > 1$. by explicit ansatz for the dipole cross section.

$$\Lambda^2_{sat}(W^2) = const \left(\frac{W^2}{1GeV^2}\right)^{C_2=0.29}$$

Normalization by $Q^2 = 0$ photoproduction (Regge fit):

$$\sigma^{(\infty)}(W^2) \cong \begin{cases} 30mb, & \text{(for 3 active flavors,)} \\ 18mb, & \text{(for 4 active flavors,)} \end{cases}$$

Simple ansatz with $\rho = 1$, $\left(R = \frac{1}{2\rho} = \frac{1}{2}\right)$:

Cvetic, Schildknecht, Surrow, Tentyukov (2001)

$$\sigma_{(q\bar{q})p}(\vec{r}_\perp, z(1-z), W^2) = \sigma^{(\infty)}(W^2)\left(1 - J_0\left(r_\perp\sqrt{z(1-z)}\Lambda_{sat}(W^2)\right)\right)$$

$$\begin{aligned} \sigma_{\gamma^* p}(W^2, Q^2) &= \sigma_{\gamma^* p}(\eta(W^2, Q^2)) + O\left(\frac{m_0^2}{\Lambda^2_{\text{sat}}(W^2)}\right) = \\ &= \frac{\alpha R_{e^+e^-}}{3\pi}\sigma^{(\infty)}(W^2) I_0(\eta) + O\left(\frac{m_0^2}{\Lambda^2_{\text{sat}}(W^2)}\right), \qquad R_{e^+e^-} = 3\sum_q Q_q^2. \end{aligned}$$

$$\begin{aligned} I_0(\eta(W^2, Q^2)) &= \frac{1}{\sqrt{1 + 4\eta(W^2, Q^2)}} \ln \frac{\sqrt{1 + 4\eta(W^2, Q^2)} + 1}{\sqrt{1 + 4\eta(W^2, Q^2)} - 1} \cong \\ &\cong \begin{cases} \ln \frac{1}{\eta(W^2, Q^2)} + O(\eta \ln \eta), & \text{for } \eta(W^2, Q^2) \to \frac{m_0^2}{\Lambda^2_{\text{sat}}(W^2)}, \\ \frac{1}{2\eta(W^2, Q^2)} + O\left(\frac{1}{\eta^2}\right), & \text{for } \eta(W^2, Q^2) \to \infty, \end{cases} \end{aligned}$$

Generalization to $\rho = \frac{4}{3}$.

Constraint: $m_0^2 \leq M_{q\bar{q}}^2, M_{q\bar{q}}'^2 \leq m_1^2(W^2)$; Kuroda, Schildknecht (2011)

$$\sigma_{\gamma^* p} = \sigma_{\gamma^* p}\left(\eta(W^2, Q^2), \frac{m_0^2}{\Lambda_{sat}^2(W^2)}, \xi \equiv \frac{m_1^2(W^2)}{\Lambda_{sat}^2(W^2)}\right),$$

$$\eta(W^2, Q^2) = \frac{Q^2 + m_0^2}{\Lambda_{sat}^2(W^2)},$$

$$\Lambda_{sat}^2(W^2) = C_1\left(\frac{W^2}{W_0^2} + 1\right)^{C_2} \cong \text{ const } \left(\frac{W^2}{1GeV^2}\right)^{C_2}$$

$$C_1 = 1.95 GeV^2$$

$$W_0^2 = 1081 GeV^2$$

$$C_2 = 0.27(0.29)$$

$$m_0^2 = 0.15 GeV^2$$

$$m_1^2(W^2) = \xi\Lambda_{sat}^2(W^2) = 130\Lambda_{sat}^2(W^2)$$

Normalization by $Q^2 = 0$ photoproduction (Regge fit):

$$\sigma^{(\infty)}(W^2) \cong \begin{cases} 30mb, & (\text{for 3 active flavors}, \quad R_{e^+e^-} = 2) \\ 18mb, & (\text{for 4 active flavors}, \quad R_{e^+e^-} = \frac{10}{3}) \end{cases}$$

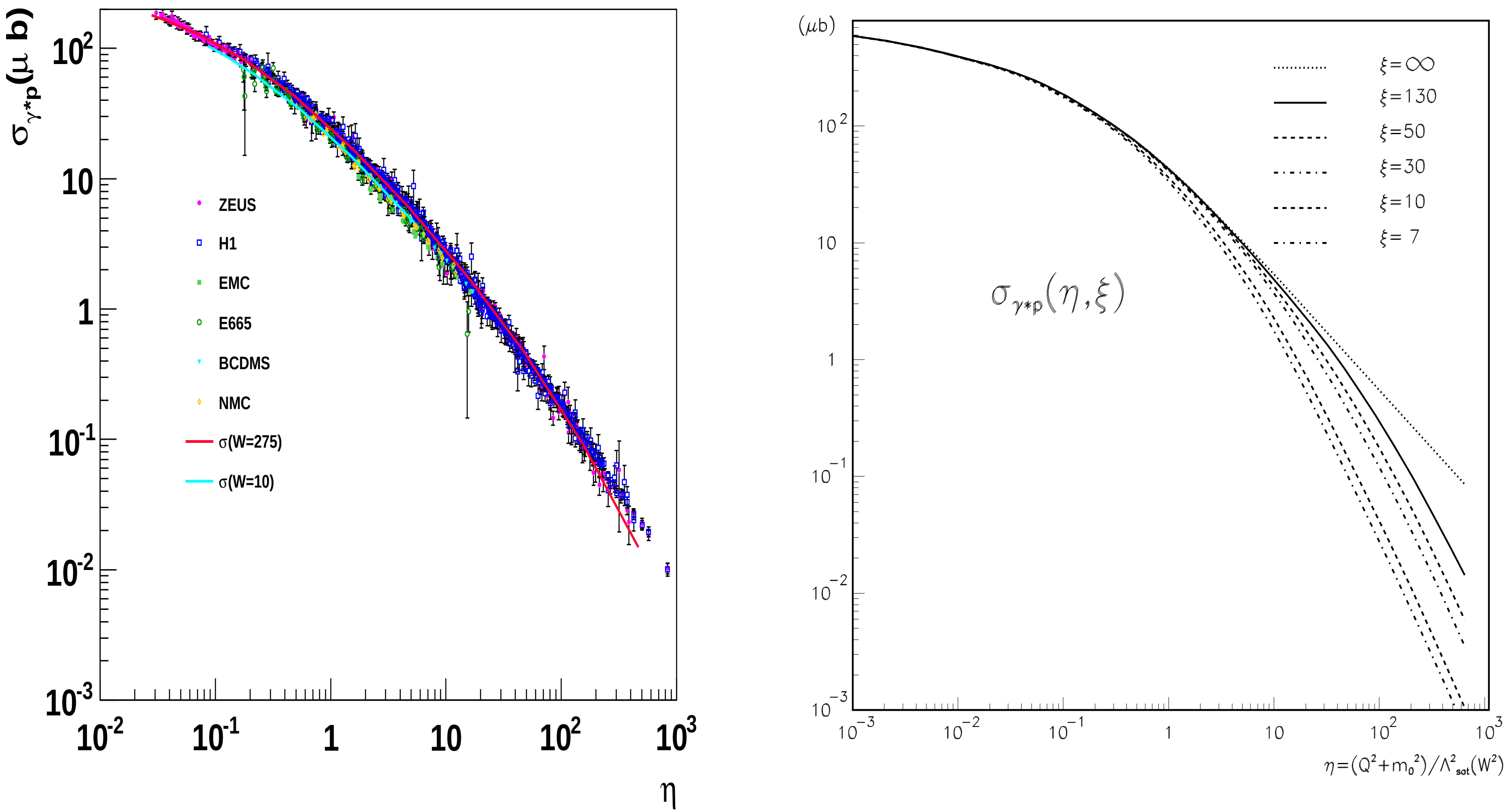

$\sigma_{\gamma^*p}(\mu\, b)$
ZEUS
H1
EMC
E665
BCDMS
NMC
σ(W=275)
σ(W=10)
η
(μb)
$\xi=\infty$
$\xi=130$
$\xi=50$
$\xi=30$
$\xi=10$
$\xi=7$
$\sigma_{\gamma * p}(\eta,\xi)$
$\eta=(Q^2+m_0^2)/\Lambda^2_{sat}(W^2)$

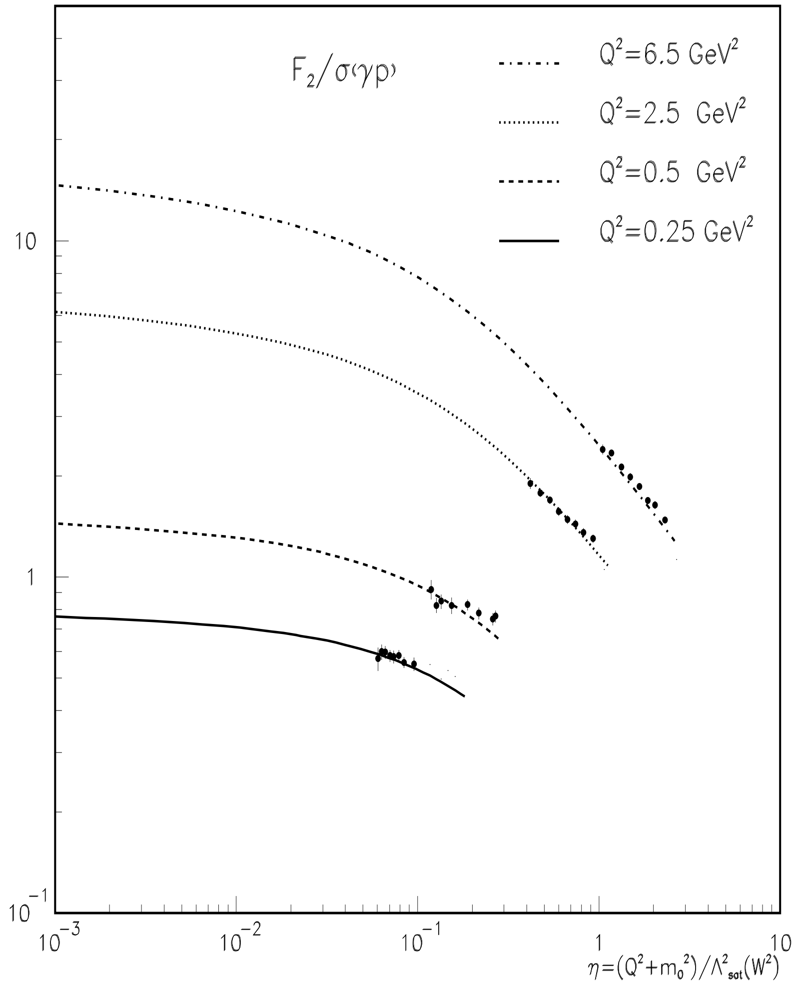

The approach to saturation.

Comparison with Caldwell 6-parameter 2 P-fit: $\sigma_{\gamma^* p} = \sigma_0 \frac{M^2}{Q^2+M^2} \left(\frac{l}{l_0}\right)^{\epsilon_0 + (\epsilon_1 - \epsilon_0)\sqrt{\frac{Q^2}{Q^2+\Lambda^2}}}$

where $$l = \frac{1}{2 x_{bj} M_p}$$

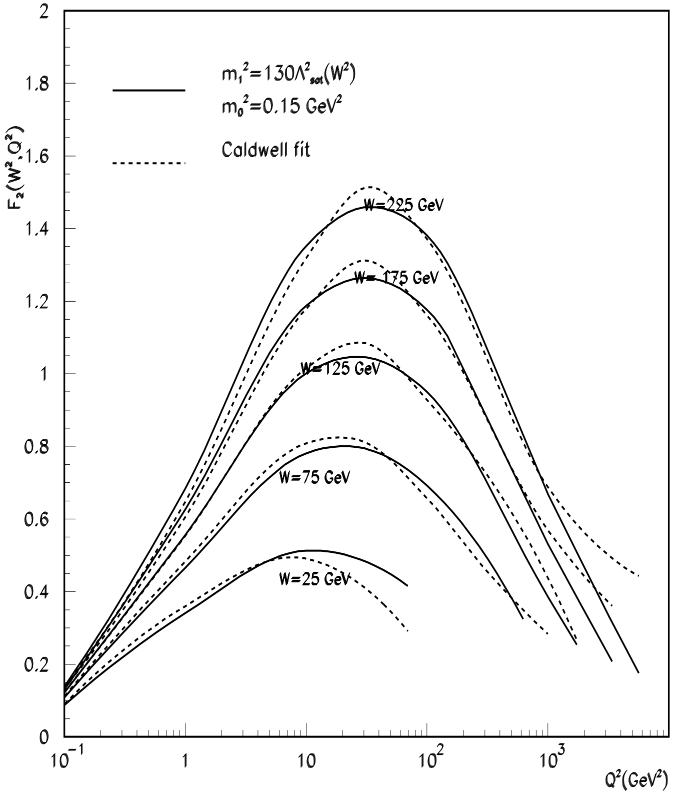

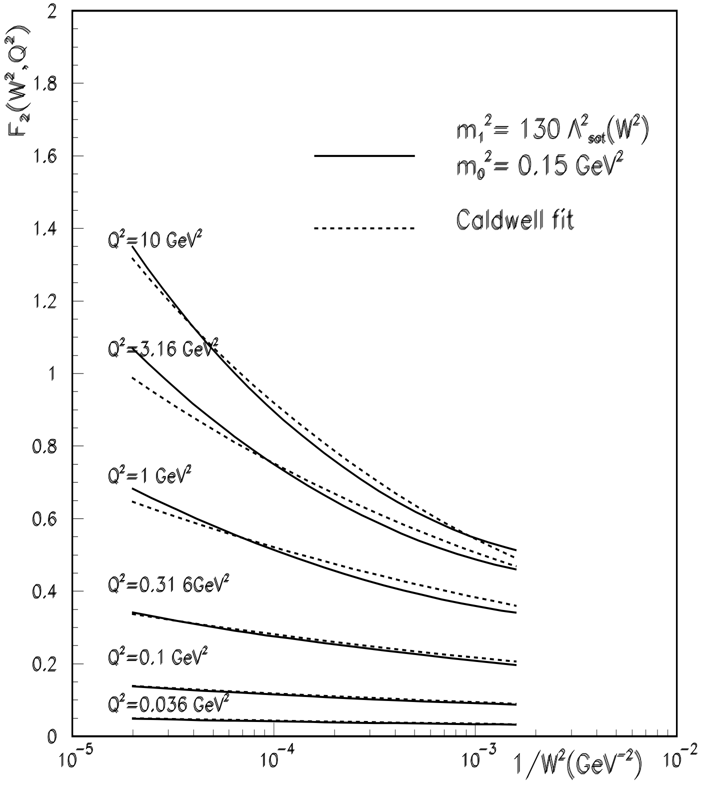

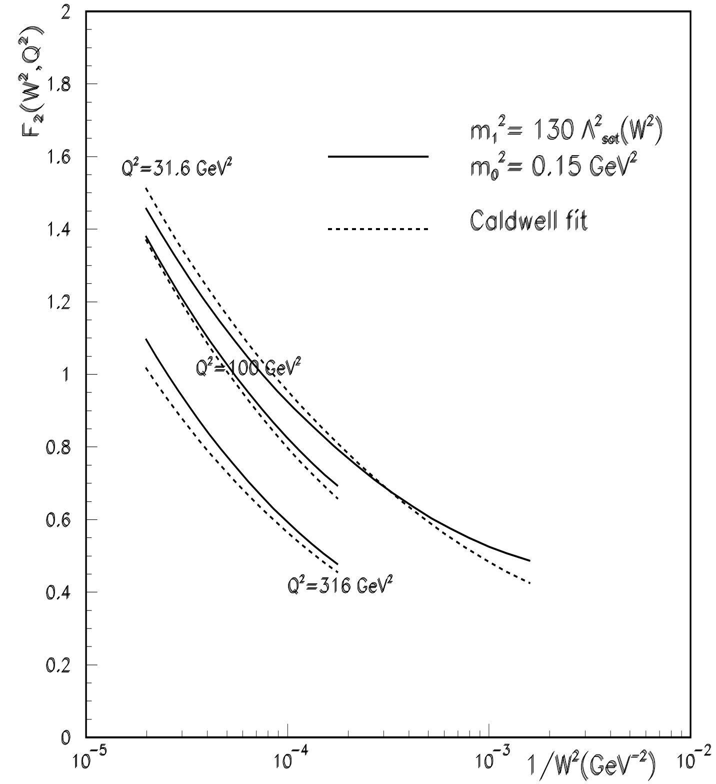

$F_2(W^2,Q^2)$
2
1.8
1.6
1.4
1.2
1
0.8
0.6
0.4
0.2
0
$m_1^2 = 130\ \Lambda^2_{sat}(W^2)$
$m_0^2 = 0.15\ GeV^2$
Caldwell fit
$Q^2=31.6\ GeV^2$
$Q^2=100\ GeV^2$
$Q^2=316\ GeV^2$
10^{-5}
10^{-4}
10^{-3}
10^{-2}
$1/W^2(GeV^{-2})$

Comparison with the experimental data directly

Prabhdeep Kaur (2010)

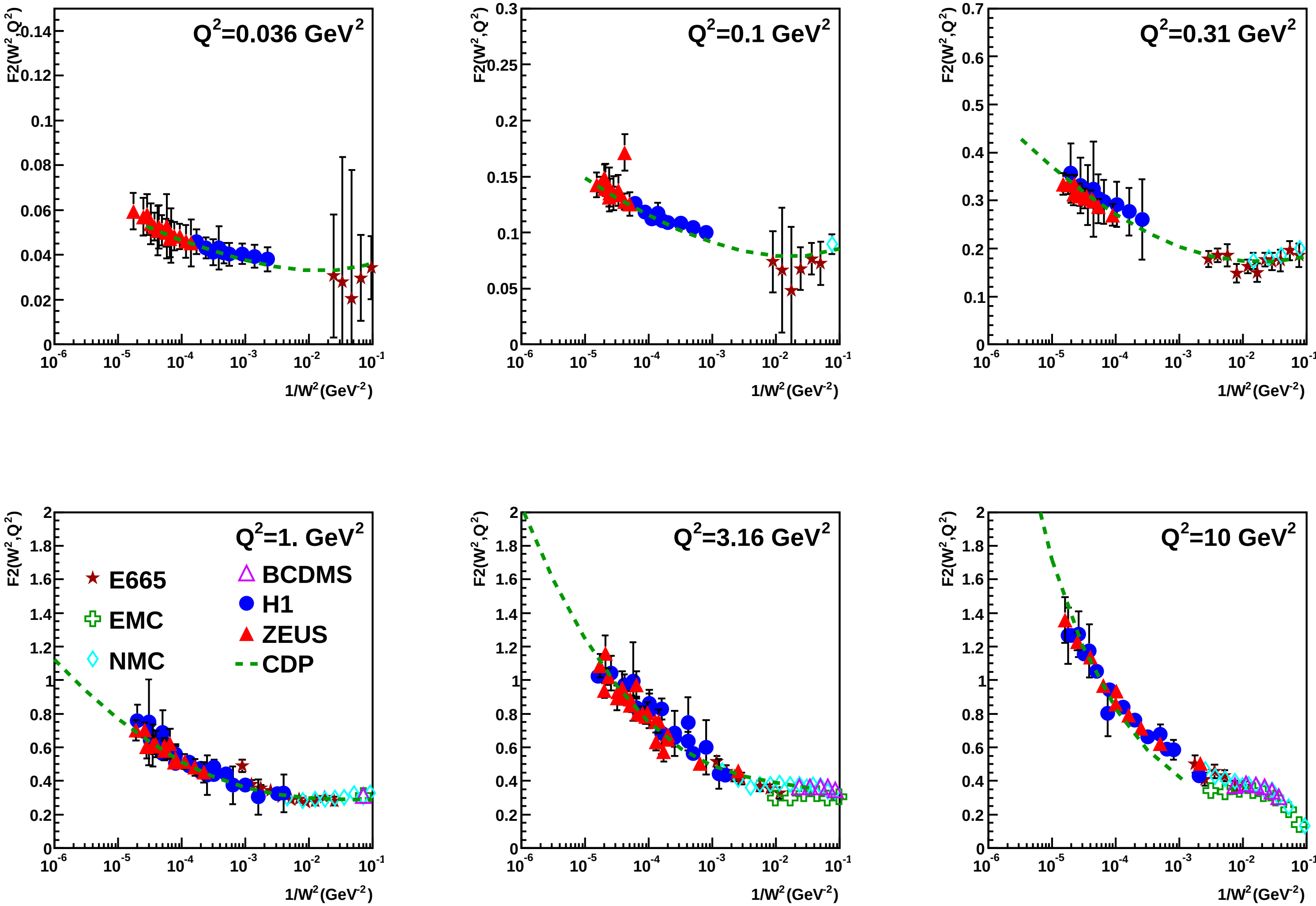

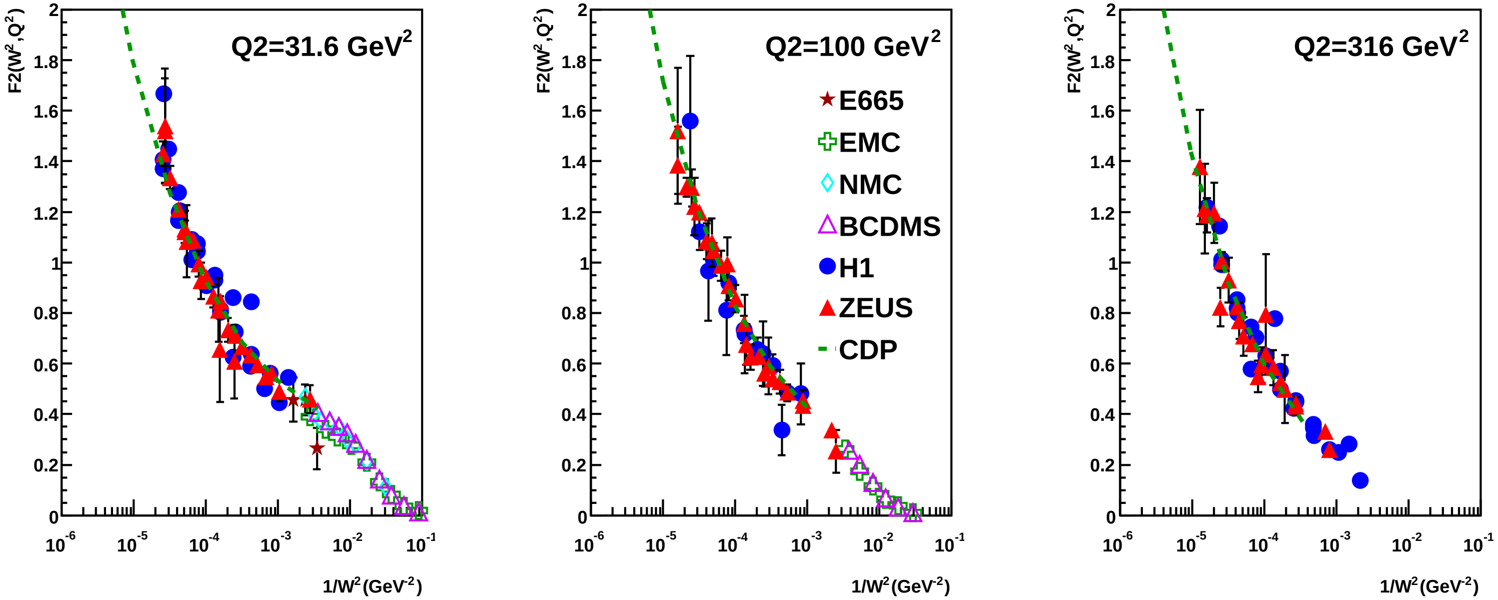
Q2=31.6 GeV^2
Q2=100 GeV^2
Q2=316 GeV^2
F2(W^2,Q^2)
1/W^2 (GeV^{-2})
E665
EMC
NMC
BCDMS
H1
ZEUS
CDP

Saturation limit: $\lim\limits_{\substack{W^2\to\infty \\ Q^2 \text{fixed}}} \frac{F_2(x \cong Q^2/W^2, Q^2)}{\sigma_{\gamma p}(W^2)} = \frac{Q^2}{4\pi^2\alpha}$

Consider $Q_1^2 = 0.036\ GeV^2$

and $Q_2^2 = 0.1 GeV^2$

$$\begin{aligned} F_2(W^2, Q_2^2 = 0.1\text{GeV}^2) &= \frac{Q_2^2}{Q_1^2} F_2(W^2, Q_1^2 = 0.036\text{GeV}^2) \\ &= 2.78 F_2(W^2, Q_1^2 = 0.036\text{GeV}^2). \end{aligned}$$

$\frac{1}{W^2}[\text{GeV}^{-2}]$	$F_2(W^2, Q_1^2 = 0.036\text{GeV}^2)$	$\frac{Q_2^2}{Q_1^2} F_2(W^2, Q_1^2 = 0.036\text{GeV}^2)$
$2 \cdot 10^{-5}$	$\cong 0.055$	0.15
10^{-4}	$\cong 0.04$	0.11

Inversion: $F_2(W^2)$ in terms of gluon distribution:

$$F_2\left(W^2 = \frac{Q^2}{x}\right) = \frac{(2\rho+1)\sum Q_q^2}{3\pi}\xi_L^{C_2}\alpha_s(Q^2)G(x,Q^2) \qquad \eta(W^2,Q^2) \gg 1.$$

$$= \frac{(2\rho+1)\sum Q_q^2}{3\pi}\frac{1}{8\pi^2}\sigma_L^{(\infty)}\Lambda_{sat}^2(W^2). \qquad \text{color transparency}$$

(upon using $F_2 = f_2\left(\frac{W^2}{1GeV^2}\right)^{0.29} = \frac{(2\rho+1)\sum Q_q^2}{3\pi}\frac{1}{8\pi^2}\sigma_L^{(\infty)}\Lambda_{sat}^2(W^2)$.)

Saturation behavior:

$$F_2(W^2,Q^2) \sim Q^2\sigma_L^{(\infty)} \ln\frac{\Lambda_{\rm sat}^2(W^2)}{Q^2+m_0^2}$$

$$\sim Q^2\sigma_L^{(\infty)} \ln\left(\frac{\alpha_s(Q^2)G(x,Q^2)}{\sigma_L^{(\infty)}(Q^2+m_0^2)}\right), \qquad \eta(W^2,Q^2) \ll 1.$$

saturation

Logarithmic dependence on gluon distribution in saturation limit.

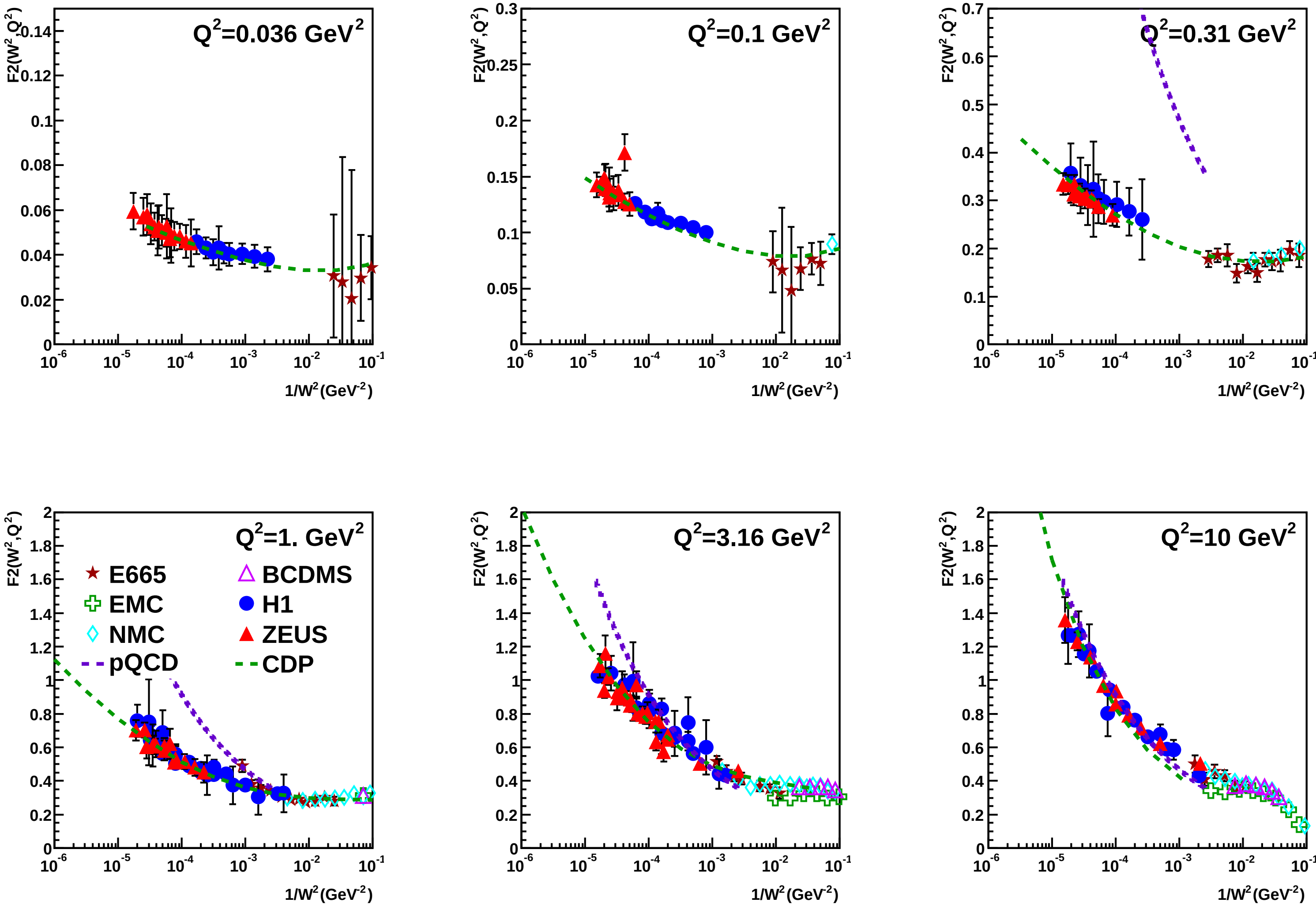

CDP and pQCD-improved parton model

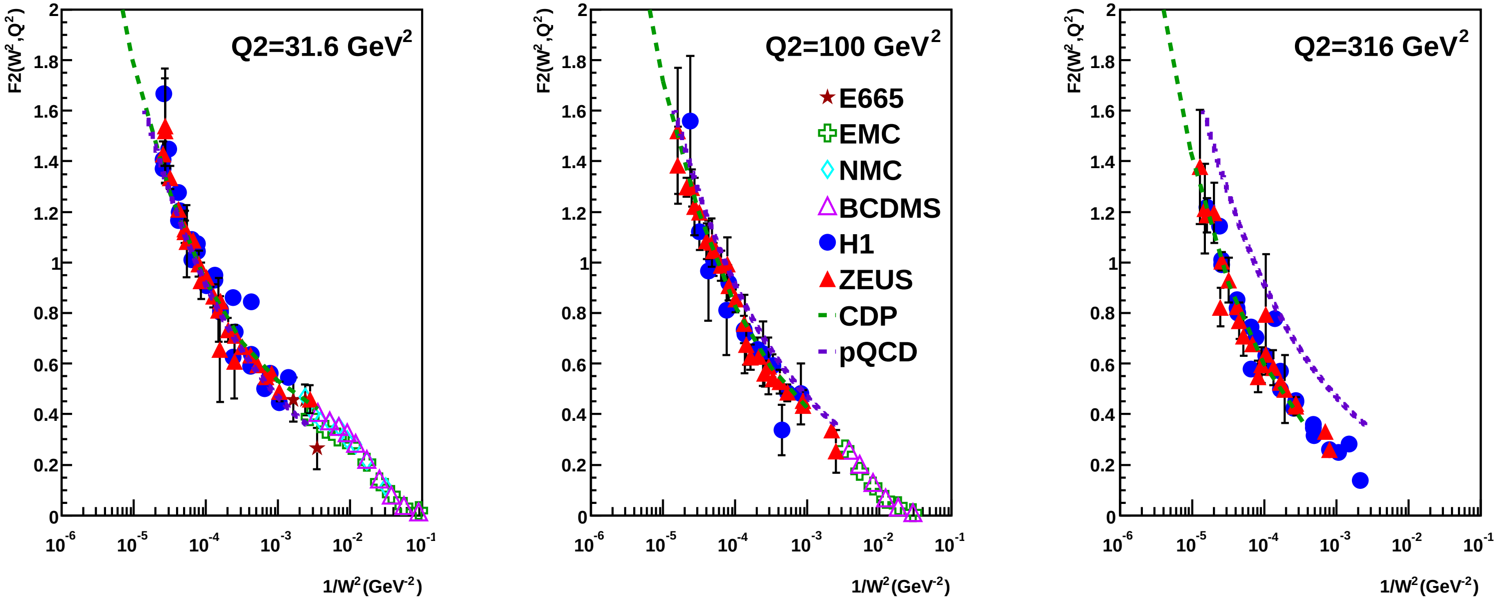

CDP and pQCD-improved parton model

The longitudinal structure function, $F_L(x, Q^2)$

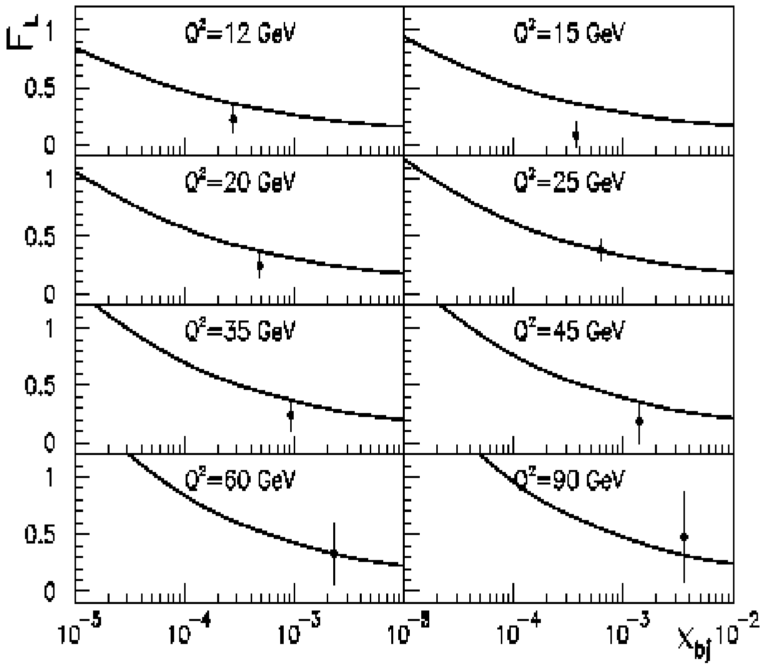

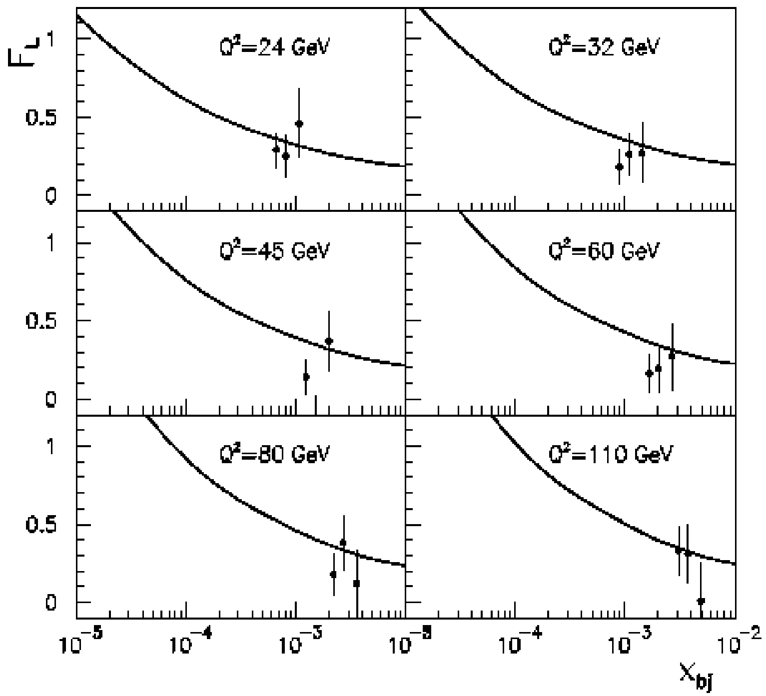

6. Conclusions

Gauge-invariant (two-gluon) interaction of color dipole:

i) Color transparency

$\sigma_{(q\bar{q})p}(\vec{r}_\perp^{\,2}, W^2) \sim \vec{r}_\perp^{\,2}$, strong cancellation between channel 1 and channel 2

relevant for $\eta(W^2, Q^2) = \frac{Q^2+m_0^2}{\Lambda^2_{sat}(W^2)} > 1$,

$\Lambda^2_{sat}(W^2) \sim (W^2)^{C_2=0.29}$

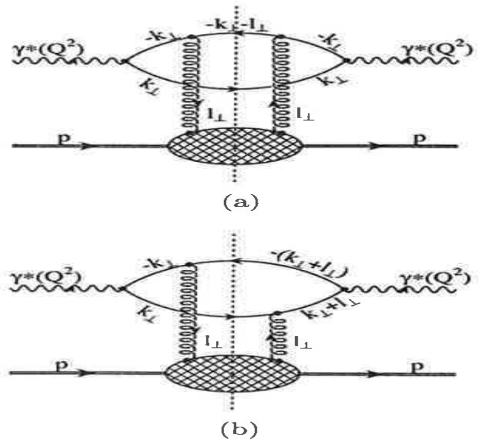

$$F_L(x, Q^2) = 0.27 F_2(x, Q^2),$$

$$\begin{aligned} F_2(x, Q^2) &= F_2(W^2 = Q^2/x) \\ &\sim \Lambda^2_{sat}(W^2)\ , \quad (10 GeV^2 < Q^2 < 100 GeV^2) \\ &\sim \alpha_s(Q^2) G(x, Q^2). \end{aligned}$$

Peaceful coexistence between CDP and pQCD-improved parton model

ii) Saturation

$\sigma_{(q\bar{q})p}(\vec{r}_\perp{}', W^2) \sim \sigma^{(\infty)}$, contribution from channel 2 has died out,

relevant for $\eta(W^2, Q^2) < 1$,

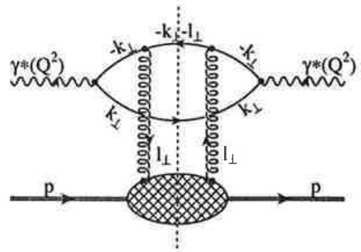

(a)

$$F_2(W^2, Q^2) \sim Q^2\sigma^{(\infty)} \ln \frac{\Lambda^2_{\mathrm{sat}}(W^2)}{Q^2 + m_0^2}$$

$$\sim Q^2\sigma^{(\infty)} \ln \left(\frac{\alpha_s(Q^2)G(x, Q^2)}{\sigma_L^{(\infty)}(Q^2 + m_0^2)} \right),$$

Smooth transition from $\eta(W^2, Q^2) \gg 1$ to $\eta(W^2, Q^2) \ll 1$, including $Q^2 = 0$.

No evidence for non-linear gluon saturation in DIS.

Concrete model, interpolating the regions of $\eta(W^2, Q^2) > 1$ and $\eta(W^2, Q^2) < 1$, describes experimental data for $x \lesssim 0.1$, including $Q^2 = 0$ photoproduction.